Hindawi
International Journal of Intelligent Systems
Volume 2024, Article ID 2140919, 24 pages
https://doi.org/10.1155/2024/2140919

WILEY | Hindawi

Research Article

A New Divergence Based on the Belief Bhattacharyya Coefficient with an Application in Risk Evaluation of Aircraft Turbine Rotor Blades

Zhu Yin, Xiaojian Ma, and Hang Wang

School of Science, Northeast Forestry University, Harbin, China

Correspondence should be addressed to Xiaojian Ma; mxjzy@nefu.edu.cn

Received 4 April 2023; Revised 6 September 2023; Accepted 22 September 2023; Published 10 January 2024

Academic Editor: Mohammad R. Khosravi

Belief divergence is a significant measure to quantify the discrepancy between evidence, which is beneficial for conflict information management in Dempster–Shafer evidence theory. In this article, three new concepts are given, namely, the belief Bhattacharyya coefficient, adjustment function, and enhancement factor. And based on them, a novel enhanced belief divergence, called EBD, is proposed, which can assess the correlation of subsets and fully reflect the uncertainty of multielement sets. The important properties of the EBD have been studied. In particular, a new EBD-based multisource information fusion method is designed to handle evidence conflict, where the weight of evidence is decided by the EBD between evidence and the information volume of each evidence. Compared with other methods, the proposed method in the applications of target recognition and iris classification can produce more rational and telling outcomes when dealing with conflict information. Finally, an application in risk priority evaluation of the failure modes of rotor blades of an aircraft turbine is provided to validate that the proposed method has the extensive applicability.

1. Introduction

Multisource information fusion is an invaluable information processing technology to achieve precise decisions by analyzing heterogeneous data from multiple sensors [1–3]. However, in practical scenarios, owing to the influence of different factors, such as bad weather conditions, mechanical failures, and wireless communication problems, the information collected from various sensors may be imprecise, incomplete, and ambiguous [4]. The Dempster–Shafer (D-S) evidence theory possesses the ability to directly express uncertain information by means of assigning basic probability assignment (BPA) to multielement sets, and can fuse evidence without the consideration of prior information to diminish the uncertainty of the system and improve its performance [5, 6]. So, it has been broadly applied in risk evaluation [7–9], output control [10], image processing [11, 12], and multicriteria decision-making [13, 14]. Nevertheless, when confronted with highly conflicting evidence, the D-S evidence theory yields counter-intuitive results [15]; then, a misdirected consequence may be brought about in a system. Therefore, how to deal with conflict is still an urgent problem in evidence theory.

To address this issue, existing research methods are primarily conducted by modifying Dempster's combination rule or preprocessing the bodies of evidence before combination [16–22]. In this article, we focus on the latter. In the study of evidence preprocessing, it is discovered that uncertainty and discrepancy measures have been extensively studied [23–28], and can be further utilized to investigate the evidence conflict. Specifically, a total uncertainty measure, based on the Euclidean distance between the belief interval of the singleton subset and the most uncertain interval, was employed to settle the conflict [29]. Cui et al. presented a plausibility entropy to measure the uncertainty of BPA [30]. Xiao presented an evidential conflict coefficient to measure the conflict between evidence [31]. Based on Tanimoto measurement, Deng devised an evidential

similarity measurement to describe the evidence inconsistency [32]. Deng et al. exploited the evidence distance to manage conflict [33]. Xiao proposed belief Jensen–Shannon (BJS) divergence to measure the discrepancy between evidence, but it is found that BJS divergence ignores the effect of multielement sets and produces measurement error [34]. Zhu et al. put forward the belief Hellinger (BH) distance and overcame the deficiency of BJS divergence [35]. Yet, BH distance differentiates multielement sets and singletons just by the cardinality of multielement sets. As for those multielement sets with same cardinality, BH distance cannot embody their difference. Specially, it is worth mentioning that Florea and Bossé gave a corrected extension of the Bhattacharyya distance based on the Bhattacharyya coefficient in probability theory to the D-S evidence theory [36]; however, the extensive form is still not mature enough to adequately reflect the diversity of evidence.

The main motivation of this study lies in the following points:

(1) In [36], Florea and Bossé's distance ignores the uncertainty of multielement sets and the interrelationship of sets, which are also the existing drawbacks of BJS divergence and BH distance, respectively. It means that a new belief divergence should be constructed to handle the uncertainty of evidence.

(2) It is significant to boost the performance of the fusion system for achieving efficient decision-making. Therefore, it is necessary to design a new algorithm to improve the accuracy of fusion.

However, there are still several challenges in this study:

(1) How to accurately reflect the uncertainty characteristics of evidence is a challenge.

(2) Designing an efficient algorithm to obtain better fusion results is a complex and challenging task.

In this paper, an enhanced belief divergence, named as EBD, is proposed to quantify the discrepancy. It fully considers the impact of multielement sets and the relationship between sets to offer a more valid solution for discrepancy measurement. The EBD satisfies the properties of boundedness, nondegeneracy, and symmetry. Based on the EBD, a new multisource information fusion algorithm is devised for conflict resolution, where the EBD determines the weights of evidence to better reflect their reliability and importance, and meanwhile, the information volume of evidence is also considered. The fusion algorithm is applied in target recognition and iris classification to evaluate its performance. Finally, the proposed method is exploited to make the risk evaluation of the rotor blades of an aircraft turbine, and verified effective and practical.

The main contributions of this study are summarized as follows:

(1) The belief Bhattacharyya coefficient and adjustment function are defined. The belief Bhattacharyya coefficient considers the uncertainty of multielement sets by the cardinality of subsets. The adjustment function can describe the correlation between different subsets. Based on the belief Bhattacharyya coefficient and influenced by the adjustment function, a new belief divergence BD is proposed and takes the uncertainty of the evidence into account.

(2) The enhancement factor is defined to promote the performance of the BD. After improvement, the enhanced belief divergence, called EBD, is presented. Compared with the other divergence and distance measures, the EBD performs discrepancy reflection more effectively.

(3) To settle conflict, an EBD-based multisource information fusion algorithm is designed, in which the EBD is employed to decide the weight of evidence. With the experiments of target recognition and iris classification to evaluate the performance and effectiveness, it demonstrates that the algorithm can achieve a more precise decision. Furthermore, the algorithm is applicable to the risk evaluation of the rotor blades of an aircraft turbine.

The paper is organized as follows. In Section 2, the preliminaries of this paper are briefly introduced. In Section 3, the belief Bhattacharyya coefficient and adjustment function are defined, and a new belief divergence BD is presented. In Section 4, based on the enhancement factor, an enhanced belief divergence EBD is proposed and its properties are proven. Furthermore, a comparative analysis is given to illustrate the validity of the EBD. In Section 5, the EBD-based multisource information fusion algorithm is designed. In Section 6, two experiments are utilized to demonstrate the effectiveness of the algorithm. In Section 7, an application in the risk priority evaluation of the failure modes of the rotor blades of an aircraft turbine demonstrates the practicality of the EBD-based fusion algorithm. Finally, conclusions are drawn in Section 8.

2. Preliminaries

In this section, some concise knowledge, including Dempster–Shafer evidence theory, base belief function, and Deng entropy, is introduced. Besides, several belief divergence and distance measures are investigated, and their inadequacies are pointed out by the examples.

2.1. Dempster–Shafer Evidence Theory. As an effective method to model and process uncertain information, the Dempster–Shafer evidence theory is primitively presented by Dempster and perfected by Shafer. [5, 6] The core concepts of it are introduced in the following.

Definition 1 (Frame of discernment). Let Θ be a finite and complete set which is composed of N mutually exclusive and collectively exhaustive hypotheses. Θ is called a frame of discernment [5, 6].

$$\Theta = \{\theta_1, \theta_2, \ldots, \theta_N\}. \quad (1)$$

The power set of Θ, consisting of all subsets of Θ, is defined as follows:

$$2^{\Theta} = \{\varnothing, \theta_1, \theta_2, \ldots, \theta_N, \{\theta_1, \theta_2\}, \ldots, \{\theta_1, \theta_2, \theta_3\}, \ldots, \Theta\}. \tag{2}$$

For any $A \subseteq \Theta$, A corresponds to a proposition. If $|A| = 1$, A is called a singleton; if $|A| > 1$, A is called a multielement set, where $|A|$ indicates the cardinality of A.

Definition 2 (Basic probability assignment). Let Θ be a frame of discernment, $\forall A \subseteq \Theta$, if a function m: $2^{\Theta} \longrightarrow [0, 1]$ satisfies the following two conditions:

$$\begin{cases} m(\varnothing) = 0, \\ \sum_{A \subseteq \Theta} m(A) = 1, \end{cases} \tag{3}$$

m is called a basic probability assignment (BPA) or mass function, [5, 6] where $m(A)$ is the support degree to proposition A. If $m(A) \neq 0$, A is called a focal element.

Definition 3 (Dempster's combination rule). Let m_1 and m_2 be two independent BPAs on Θ, $m = m_1 \oplus m_2$ is a new evidence after combination between m_1 and m_2. Dempster's combination rule is defined as follows [5, 6]:

$$\begin{cases} m(\varnothing) = 0, \\ m(A) = \dfrac{1}{1-k} \sum_{A=B \cap C} m_1(B) m_2(C), \end{cases} \tag{4}$$

where $B, C \subseteq \Theta$ and $k = \sum_{B \cap C = \varnothing} m_1(B) m_2(C)$ is called conflict coefficient, k satisfies $0 \leq k < 1$.

2.2. Base Belief Function. Base belief function is primarily proposed to address the fusion problem of highly conflicting evidence [37]. In this paper, base belief function is flexibly utilized to solve zero belief value by modifying the evidence.

Definition 4 (Base belief function). Let Θ be a frame of discernment, composed of N mutually exclusive and collectively exhaustive hypotheses. The power set of Θ contains 2^N propositions, for every proposition $A_i (i = 1, \ldots, 2^N)$ in 2^{Θ} except $\varnothing$, base belief function is defined as follows [37]:

$$m_b(A_i) = \frac{1}{2^N - 1}. \tag{5}$$

2.3. Deng Entropy. The uncertainty of BPA is considered beneficial for handling conflict, therefore, a quantity of uncertainty measures have been explored from different perspectives [38, 39]. As the extension of Shannon entropy, the Deng entropy is proposed to represent the uncertainty of evidence. The Deng entropy is denoted as in [40].

$$E_d = -\sum_{A \subseteq \Theta} m(A) \log_2 \frac{m(A)}{2^{|A|} - 1}, \tag{6}$$

where $A \subseteq \Theta$ and $|A|$ is cardinal number of A.

2.4. Divergence and Distance Measures. In D-S evidence theory, how to choose an appropriate method to determine the difference between evidence is still an open issue. To date, a score of discrepancy measures have been developed [41, 42]. In this section, Bhattacharyya distance, Florea and Bossé's distance, belief Jenson–Shannon divergence, and belief Hellinger distance are introduced.

In statistics, the Bhattacharyya distance is utilized to measure the similarity between two probability distributions, and it is closely related to the Bhattacharyya coefficient which is used to calculate the overlap degree between samples [43]. Bhattacharyya distance is defined as follows.

Definition 5 (Bhattacharyya distance). Given two probability distributions $P = (p_1, \ldots, p_n)$ and $Q = (q_1, \ldots, q_n)$ with $\sum_i p_i = \sum_i q_i = 1$, Bhattacharyya distance is defined as $-\ln(\mathrm{BC})$, where BC is the Bhattacharyya coefficient and denoted by [43]

$$\mathrm{BC}(p, q) = \sum_{i=1}^{n} \sqrt{p_i q_i}. \tag{7}$$

BC satisfies $0 \leq \mathrm{BC}(p, q) \leq 1$.

Ristic and Smets put forward the extension of Bhattacharyya distance from probability theory to D-S evidence theory [44]. By correcting the above distance, Florea and Bossé's distance is given by [36]

$$d_B(m_1, m_2) = \left[1 - \sum_{A \subseteq \Theta} \sqrt{m_1(A) m_2(A)}\right]^p, \tag{8}$$

where m_1 and m_2 are two independent BPAs defined on Θ and p could be any positive number.

In this paper, we only pay attention to the case of $p = 1/2$, namely, $d_B(m_1, m_2) = [1 - \sum_{A \subseteq \Theta} \sqrt{m_1(A) m_2(A)}]^{1/2}$.

Nevertheless, Florea and Bossé's distance is immature to accurately reflect evidence difference. In other words, Florea and Bossé's distance is unable to differentiate between probability distribution and BPA without considering the uncertainty carried by BPA.

Xiao incorporated Jensen–Shannon divergence into evidence theory and proposed a novel belief divergence, which is presented as follows [34].

Definition 6 (Belief Jensen–Shannon divergence). Given two independent BPAs m_1 and m_2 defined on Θ, belief Jensen–Shannon (BJS) divergence between m_1 and m_2 is defined as follows [34]:

$$\mathrm{BJS}(m_1, m_2) = \frac{1}{2}\left[\sum_i m_1(A_i)\log\frac{2m_1(A_i)}{m_1(A_i)+m_2(A_i)} + \sum_i m_2(A_i)\log\frac{2m_2(A_i)}{m_1(A_i)+m_2(A_i)}\right], \tag{9}$$

where $\sum_i m_j(A_i) = 1$, $(i = 1, \ldots, n; j = 1, 2)$.

BJS divergence has a preferable effect on describing the deviation between evidence, but it fails to recognize the multielement sets. This restriction is illustrated by Example 1.

Example 1. Suppose m_1, m_2, and m_3 are three independent BPAs defined on $\Theta = \{A, B\}$.

$$\begin{aligned} &m_1\colon m_1(\{A\}) = 0.80, m_1(\{B\}) = 0.10, m_1(\{A, B\}) = 0.10;\\ &m_2\colon m_2(\{A\}) = 0.10, m_2(\{B\}) = 0.80, m_2(\{A, B\}) = 0.10;\\ &m_3\colon m_3(\{A\}) = 0.10, m_3(\{B\}) = 0.10, m_3(\{A, B\}) = 0.80. \end{aligned} \tag{10}$$

Intuitively, m_1 strongly supports $\{A\}$ and m_2 strongly supports $\{B\}$, so m_1 and m_2 are highly conflicting. m_3 supports the proposition $\{A, B\}$, which represents a uncertain state to support A or B. Therefore, the divergence between m_1 and m_2 is the largest amongst all evidence, the divergence between m_3 and m_2 is identical with that between m_3 and m_1. However, according to equation (9), the results are calculated as follows:

$$\mathrm{BJS}(m_1, m_2) = 0.4471, \mathrm{BJS}(m_1, m_3) = 0.4471, \mathrm{BJS}(m_2, m_3) = 0.4471. \tag{11}$$

Obviously, it is not consistent with the intuition. The reason for such counter-intuitive results is that BJS divergence neglects the multielement subset $\{A, B\}$ with uncertainty by treating it as a singleton.

Generalized from the Hellinger distance of probability theory, belief Hellinger distance, which overcomes the defect of BJS divergence, is defined as follows [35].

Definition 7 (Belief Hellinger distance). Let m_1 and m_2 be two independent BPAs defined on Θ, belief Hellinger (BH) distance between m_1 and m_2 is defined as follows [35]:

$$\mathrm{BH}(m_1, m_2) = \frac{1}{\sqrt{2}}\sqrt{\sum_{i=1}^{n}\frac{\left(\sqrt{m_1(A_i)} - \sqrt{m_2(A_i)}\right)^2}{2^{|A_i|}-1}}, \tag{12}$$

where $A_i \in 2^\Theta$, $|A_i|$ is cardinal number of A_i.

From (12), BH distance takes the cardinal number of subset into account, so multielement set can be distinguished from singleton by the size difference. Recalculate Example 1 by BH distance, the results are obtained as follows:

$$\mathrm{BH}(m_1, m_2) = 0.5782, \mathrm{BH}(m_1, m_3) = 0.4721, \mathrm{BH}(m_2, m_3) = 0.4721. \tag{13}$$

In comparison with BJS divergence, the above results by BH distance are more reasonable. Nevertheless, BH cannot embody the correlation between hypotheses contained in different subsets. Explicitly, if the cardinality of all multielement sets is designed as the same, BH distance is unable to identify the difference between these sets, which have the same cardinality but different elements. This situation will be vividly illustrated by Example 2.

Example 2. Suppose m_1, m_2, and m_3 are three independent BPAs defined on $\Theta = \{A, B, C, D\}$.

$$\begin{aligned} &m_1\colon m_1(\{A\}) = 0.30, m_1(\{B\}) = 0.40, m_1(\{A, B\}) = 0.30;\\ &m_2\colon m_2(\{A\}) = 0.30, m_2(\{B\}) = 0.40, m_2(\{A, C\}) = 0.30;\\ &m_3\colon m_3(\{A\}) = 0.30, m_3(\{B\}) = 0.40, m_3(\{C, D\}) = 0.30. \end{aligned} \tag{14}$$

It can be seen that m_1, m_2, and m_3 all support the proposition $\{B\}$. Meanwhile, the cardinality of multielement sets, $\{A, B\}$, $\{A, C\}$, and $\{C, D\}$, in three evidence is identical, and the difference of three evidence is only that of hypotheses included in them. Specifically, $\{A, B\}$ in m_1 are probable to distribute its belief to hypothesis A or B, so m_1

may have further possibility to support B. $\{A, C\}$ in m_2 has more probability to support A. Dissimilarly, $\{C, D\}$ in m_3 does not have any likelihood to support A and B. From above analysis, BH distance between evidence should satisfy $\mathrm{BH}(m_1, m_2) < \mathrm{BH}(m_2, m_3) < \mathrm{BH}(m_1, m_3)$. However, by equation (12), the results are calculated as follows:

$$\mathrm{BH}(m_1, m_2) = 0.3162, \mathrm{BH}(m_1, m_3) = 0.3162, \mathrm{BH}(m_2, m_3) = 0.3162. \tag{15}$$

Apparently, BH distance does not change, which is insufficient as an evidence distance measure. Therefore, it is needed to find a more reliable and stable belief discrepancy measure.

3. A New Belief Divergence Measure

In this section, the belief Bhattacharyya coefficient is presented. In addition, an adjustment function is defined. Based on the belief Bhattacharyya coefficient and affected by the adjustment function, a new belief divergence is proposed to signify the discrepancy between evidence.

In order to reflect the impact of multielement sets, it is considered that the cardinality factor can tell the multielement sets from singletons. Attributed to this peculiarity, the belief Bhattacharyya coefficient is proposed as follows.

Definition 8 (belief Bhattacharyya coefficient). Let m_1 and m_2 be two mass functions on Θ, the belief Bhattacharyya coefficient (BBC) between m_1 and m_2 is defined as follows:

$$\mathrm{BBC}(m_1, m_2) = \sum_{i=1}^{n} \frac{\sqrt{m_1(A_i) m_2(A_i)}}{2^{|A_i|} - 1}. \tag{16}$$

According to the boundedness of Bhattacharyya coefficient, the belief Bhattacharyya coefficient also satisfies $0 \le \mathrm{BBC}(m_1, m_2) \le 1$.

In addition, the Bhattacharyya coefficient can be denoted as fidelity; the physical significance of fidelity is the inner product of two probability vectors on a sphere, representing the similarity between two probability distributions [45]. The belief Bhattacharyya coefficient can be seen as a generalization of fidelity in Dempster–Shafer theory. In [45], another extension of fidelity called FBIP has been proposed. To demonstrate the meaningfulness and value of our extension, a comparative experiment between BBC and FBIP is conducted in Example 3.

Example 3. Suppose m_1 and m_2 are two independent BPAs defined on $\Theta = \{A, B, C, D\}$, where x ranges from 0 to 1.

$$\begin{aligned} &m_1\colon m_1(\{A\}) = 1, m_1(\{B\}) = 0, m_1(\{C, D\}) = 0; \\ &m_2\colon m_2(\{A\}) = x, m_2(\{B\}) = 0, m_2(\{C, D\}) = 1 - x. \end{aligned} \tag{17}$$

Figure 1 depicts the change of the BBC and FBIP as x uniformly increases from 0 to 1 with an increment of $\Delta = 0.01$. As x gradually increases, m_1 and m_2 become more similar, leading to an increase in both BBC and FBIP. Specifically, at $x = 0$, m_1 and m_2 are completely conflicting, resulting in a similarity of 0; at $x = 1$, the evidence distributions are identical, yielding a similarity of 1. Overall, the change of BBC is relatively uniform, and the change of FBIP becomes significantly less pronounced after $x > 0.6$. Therefore, the BBC exhibits better measurement characteristics.

In order to reveal the relationship between sets, it is learned that the transformation factor G in [46] can measure the intersection relationship between focal elements, [46] but we find that, the sum of the transformed mass function may be greater than 1, which spoils the nature of BPA. Hence, by the normalization of each row of the transformation factor, a new adjustment function is defined as follows.

Definition 9 (adjustment function). Let m_1 and m_2 be two mass functions on Θ including N hypotheses. $\{A_1, A_2, \ldots, A_n\}$ is a set of n focal elements, adjustment function is defined as

$$\Gamma_{A_i, A_j} = \frac{\left(2^{|A_i \cap A_j|} - 1\right) / \left(2^{|A_i \cup A_j|} - 1\right)}{\sum_{j=1}^{n} \left(2^{|A_i \cap A_j|} - 1\right) / \left(2^{|A_i \cup A_j|} - 1\right)}, \quad i, j = 1, 2, \ldots, n. \tag{18}$$

Adjustment function Γ is the ratio of the interaction degree between A_i and A_j to the whole sum of that between A_i and all focal elements, which implies the importance of A_j in all interaction relationships of A_i. In other words, Γ_{A_i, A_j} is the ratio of the belief that A_i assigns to A_j relative to the belief of A_i itself. Therefore, Γ_{A_i, A_j} not only retains the primary property of BPA, namely, the sum of modified BPA with Γ is 1 but also has the ability to express the contribution difference of different subsets to the supportive proposition of evidence.

In Example 2, intuitively, the supportive proposition in m_1 and m_3 is $\{B\}$, the contribution degree of $\{A, B\}$ to $\{B\}$ in m_1 is greater than that of $\{C, D\}$ to $\{B\}$ in m_3. By (18), the adjustment function $\Gamma_{\{B\}, \{A, B\}}$ in m_1 is 1/4, the adjustment function $\Gamma_{\{B\}, \{C, D\}}$ in m_3 is 0, which is in conformity with the intuition.

Based on the BBC and Γ, a new belief divergence, considering the uncertainty of multielement sets and the correlation between subsets, is proposed. Its detailed definition is as follows.

Definition 10 (the belief divergence BD). Given two independent BPAs m_1 and m_2 defined on Θ including N hypotheses, $\{A_1, A_2, \ldots, A_n\}$ is a set of n focal elements, satisfying $m_1(A_i) \neq 0 \vee m_2(A_i) \neq 0, A_i \in 2^{\Theta}$, the belief divergence is defined as follows:

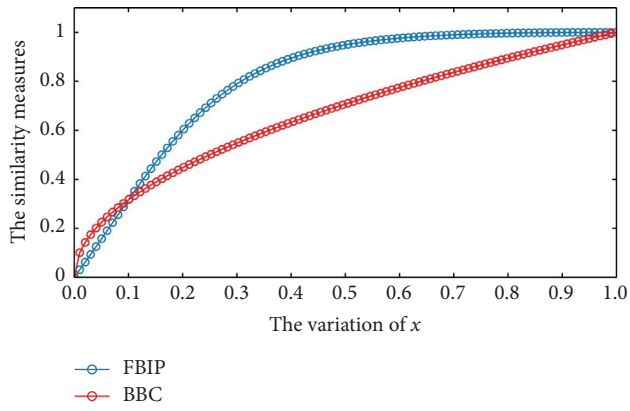

Figure 1: The comparison of the BBC and FBIP.

$$\mathrm{BD}(m_1, m_2) = \sqrt{1 - \frac{\mathrm{BBC}\left({}^{\Gamma}m_1, {}^{\Gamma}m_2\right)}{\mathrm{BBC}\left({}^{\Gamma}m_1, {}^{\Gamma}m_1\right) + \mathrm{BBC}\left({}^{\Gamma}m_2, {}^{\Gamma}m_2\right) - \mathrm{BBC}\left({}^{\Gamma}m_1, {}^{\Gamma}m_2\right)}}, \tag{19}$$

where $\mathrm{BBC}({}^{\Gamma}m_1, {}^{\Gamma}m_2) = \sum_{i=1}^{n} \sqrt{{}^{\Gamma}m_1(A_i)\,{}^{\Gamma}m_2(A_i)}/(2^{|A_i|} - 1)$, $i = 1, 2, \ldots, n$. ${}^{\Gamma}m_1$ and ${}^{\Gamma}m_2$ are new BPAs after m_1 and m_2 are modified by adjustment function, the concrete modification process is displayed as follows:

$$\begin{cases} {}^{\Gamma}m_1(A_i) = \sum_{j=1}^{n} m_1(A_j)\Gamma_{A_j, A_i}, \\ {}^{\Gamma}m_2(A_i) = \sum_{j=1}^{n} m_2(A_j)\Gamma_{A_j, A_i}. \end{cases} \tag{20}$$

Here, we provide additional explanations to illustrate the divergence. The divergence measure is utilized to reflect the variation of information distribution and can be seen as an extension of the uncertainty measure. The information quality IQ (p) proposed by Yager is the negation of the Gini index; both of them are uncertainty measures [47, 48]. The Bhattacharyya coefficient BC can be seen as a similarity measure of the IQ (p) in [47] or Gini index in [48]. Li extended IQ (p) to the information quality IQ (m) under the framework of evidence theory [49]. The belief Bhattacharyya coefficient BBC, a generalization of the Bhattacharyya coefficient, can be seen as a similarity measure of the IQ (m). Therefore, the BD based on the BBC can be seen as a belief divergence of the IQ (m).

Recall Examples 1 and 2, where the divergence measure among m_1, m_2, and m_3 is recalculated by BD, which is compared with BJS divergence and BH distance in Table 1. From Table 1, different with the unreasonable results by BJS divergence and BH distance, it is uncovered that in Example 1, $\mathrm{BD}(m_1, m_2) > \mathrm{BD}(m_1, m_3) = \mathrm{BD}(m_2, m_3)$, in Example 2, $\mathrm{BD}(m_1, m_3) > \mathrm{BD}(m_2, m_3) > \mathrm{BD}(m_1, m_2)$. The BD is more accurate to measure the conflict between evidence.

4. The Enhanced Belief Divergence

The BD does reflect the degree of conflict between evidence from diverse sources and has vanquished the demerits of BJS divergence and BH distance. Notably, it appears that the divergence measures of all groups of evidence, respectively, in the first case of zero belief value and the second case of the same cardinality, are the same. To address this limitation, an enhancement factor is proposed, and a base belief function is used to reinforce the BD; that is, an enhanced belief divergence EBD is presented. Besides, the properties of the EBD have been discussed. Finally, a comparative evaluation is given to illustrate the validity and superiority of the EBD.

4.1. Modification with the Base Belief Function. From the operational property of the BBC, it is observed that the BD may fail in measuring the discrepancy of evidence, when evidence has a zero belief value. The nature of this phenomenon is concretely illustrated by the Case 11.

Case 11. Suppose m_1 and m_2, m_3 and m_4 are two groups of BPAs defined on $\Theta = \{A, B, C, D\}$.

$$\begin{aligned} &\text{Group 1} \begin{cases} m_1(\{A\}) = 0.7, m_1(\{B\}) = 0, m_1(\{C\}) = 0.3, \\ m_2(\{A\}) = 0, m_2(\{B\}) = 1, m_2(\{C\}) = 0, \end{cases} \\ &\text{Group 2} \begin{cases} m_3(\{A\}) = 0.7, m_3(\{B, C\}) = 0, m_3(\{D\}) = 0.3, \\ m_4(\{A\}) = 0, m_4(\{B, C\}) = 1, m_4(\{D\}) = 0. \end{cases} \end{aligned} \tag{21}$$

In group 1, m_1 and m_2 are conflicting. In group 2, because of the uncertainty of the multielement set $\{B, C\}$ in m_4, the conflict degree between m_3 and m_4 is smaller than that of

Table 1: The results comparison with BJS divergence in Example 1 and BH distance in Example 2.

Examples	Discrepancy measure	BD
Example 1	$\mathrm{BJS}(m_1, m_2) = 0.4471$	$\mathrm{BD}(m_1, m_2) = 0.6646$
	$\mathrm{BJS}(m_1, m_3) = 0.4471$	$\mathrm{BD}(m_1, m_3) = 0.4123$
	$\mathrm{BJS}(m_2, m_3) = 0.4471$	$\mathrm{BD}(m_2, m_3) = 0.4123$
Example 2	$\mathrm{BH}(m_1, m_2) = 0.3162$	$\mathrm{BD}(m_1, m_2) = 0.1868$
	$\mathrm{BH}(m_1, m_3) = 0.3162$	$\mathrm{BD}(m_1, m_3) = 0.3865$
	$\mathrm{BH}(m_2, m_3) = 0.3162$	$\mathrm{BD}(m_2, m_3) = 0.2638$

group 1. By equation (20), both groups of modified BPAs are obtained as follows:

$$\begin{aligned} \text{Group 1} &\begin{cases} {}^{\Gamma}m_1\colon\ (0.7, 0, 0.3), \\ {}^{\Gamma}m_2\colon\ (0, 1, 0), \end{cases} \\ \text{Group 2} &\begin{cases} {}^{\Gamma}m_3\colon\ (0.7, 0, 0.3), \\ {}^{\Gamma}m_4\colon\ (0, 1, 0). \end{cases} \end{aligned} \tag{22}$$

According to equation (16), we have

$$\begin{aligned} \mathrm{BBC}\left({}^{\Gamma}m_1, {}^{\Gamma}m_2\right) &= 0, \\ \mathrm{BBC}\left({}^{\Gamma}m_3, {}^{\Gamma}m_4\right) &= 0. \end{aligned} \tag{23}$$

Then, according to equation (19), the BD is calculated as follows:

$$\begin{aligned} \mathrm{BD}\left(m_1, m_2\right) &= 1, \\ \mathrm{BD}\left(m_3, m_4\right) &= 1. \end{aligned} \tag{24}$$

From the above result, the degree of conflict of the two groups is the same. It is counterintuitive. Actually, as for each focal element of ${}^{\Gamma}m_1$ and ${}^{\Gamma}m_2$, if its belief value in ${}^{\Gamma}m_1$ or ${}^{\Gamma}m_2$ is 0, the BBC is 0, then the BD is always equal to 1 in this situation.

It is noticed that Liu exploited the base belief function to handle a possible zero in the denominator of the divergence [46]. Inspired by it, in this paper, for resolving zero belief, we modify the ${}^{\Gamma}m$ by averaging it and m_b to obtain ${}^{\Gamma}_{b}m$, then belief of all focal elements in ${}^{\Gamma}_{b}m$ is made nonzero. Thus, the Case 11 for the BD is managed.

4.2. The Enhancement Factor. In addition, it is found from (19) that when all focal elements of two pieces of evidence have the same cardinality, the influence of cardinality will be offset by the fractional term $\mathrm{BBC}({}^{\Gamma}m_1, {}^{\Gamma}m_2)/[\mathrm{BBC}({}^{\Gamma}m_1, {}^{\Gamma}m_1) + \mathrm{BBC}({}^{\Gamma}m_2, {}^{\Gamma}m_2) - \mathrm{BBC}({}^{\Gamma}m_1, {}^{\Gamma}m_2)]$. This is interpreted in detail by Case 12.

Case 12. Suppose m_1 and m_2, m_3 and m_4, and m_5 and m_6 are three groups of BPAs defined on $\Theta = \{\theta_1, \theta_2, \theta_3, \theta_4, \theta_5, \theta_6\}$.

$$\begin{aligned} \text{Group 1} &\begin{cases} m_1(\{\theta_1\}) = 0.90, m_1(\{\theta_2\}) = 0.10, \\ m_2(\{\theta_1\}) = 0.10, m_2(\{\theta_2\}) = 0.90, \end{cases} \\ \text{Group 2} &\begin{cases} m_3(\{\theta_1, \theta_2\}) = 0.90, m_3(\{\theta_3, \theta_4\}) = 0.10, \\ m_4(\{\theta_1, \theta_2\}) = 0.10, m_4(\{\theta_3, \theta_4\}) = 0.90, \end{cases} \\ \text{Group 3} &\begin{cases} m_5(\{\theta_1, \theta_2, \theta_3\}) = 0.90, m_5(\{\theta_4, \theta_5, \theta_6\}) = 0.10, \\ m_6(\{\theta_1, \theta_2, \theta_3\}) = 0.10, m_6(\{\theta_4, \theta_5, \theta_6\}) = 0.90. \end{cases} \end{aligned} \tag{25}$$

In this example, each group of evidence is highly conflicting. With the cardinality of subsets enlarging, m_5 and m_6 in group 3 carry the largest ambiguity. Therefore, the divergence between m_5 and m_6 is the smallest, and that between m_1 and m_2 is the largest. Whereas, by applying the BD, we obtain the divergences as follows:

$$\begin{aligned} \mathrm{BD}\left(m_1, m_2\right) &= 0.7559, \\ \mathrm{BD}\left(m_3, m_4\right) &= 0.7559, \\ \mathrm{BD}\left(m_5, m_6\right) &= 0.7559. \end{aligned} \tag{26}$$

The above result is not in line with the intuitive analysis. The reason for this is that the item $1/(2^{|A_i|} - 1)$ in equation (19) appears in both the numerator and denominator of $\mathrm{BBC}({}^{\Gamma}m_1, {}^{\Gamma}m_2)/[\mathrm{BBC}({}^{\Gamma}m_1, {}^{\Gamma}m_1) + \mathrm{BBC}({}^{\Gamma}m_2, {}^{\Gamma}m_2) - \mathrm{BBC}({}^{\Gamma}m_1, {}^{\Gamma}m_2)]$. When the cardinality of all focal elements in each group is the same, the fractional expression makes the influence of $|A_i|$ eliminated.

To deal with this case, an enhancement factor is devised to perfect the measure effect of the BD, which is defined as follows.

Definition 13 (the enhancement factor β). Given two independent BPAs m_1 and m_2 defined on Θ including N hypotheses, $\{A_1, A_2, \ldots, A_n\}$ is a set of n focal elements satisfying $m_1(A_i) \neq 0 \vee m_2(A_i) \neq 0, A_i \in 2^{\Theta}$, the enhancement factor β is denoted as follows:

$$\beta = \begin{cases} 1, & \text{else}, \\ \dfrac{1}{c}, & \forall |A_i| = c\,(c \geq 2), m_1(A_i) \neq 0 \vee m_2(A_i) \neq 0, \quad i = 1, 2, \ldots, n. \end{cases} \tag{27}$$

As can be seen in (27), the enhancement factor considers the ambiguity difference by various values of c. Thus, by it, the BD can distinguish evidence conflict degree of the Case 2.

4.3. The Enhanced Belief Divergence. With the enhancement factor and base belief function, the enhanced belief divergence EBD is proposed.

Definition 14 (the enhanced belief divergence EBD). Given two independent BPAs m_1 and m_2 defined on Θ including N hypotheses. $\{A_1, A_2, \ldots, A_n\}$ is a set of n focal elements satisfying $m_1(A_i) \neq 0 \vee m_2(A_i) \neq 0, A_i \in 2^\Theta$. The enhanced belief divergence EBD is defined as follows:

$$\mathrm{EBD}(m_1, m_2) = \beta \times \sqrt{1 - \frac{\mathrm{BBC}\left({}^{\Gamma}_{b}m_1, {}^{\Gamma}_{b}m_2\right)}{\mathrm{BBC}\left({}^{\Gamma}_{b}m_1, {}^{\Gamma}_{b}m_1\right) + \mathrm{BBC}\left({}^{\Gamma}_{b}m_2, {}^{\Gamma}_{b}m_2\right) - \mathrm{BBC}\left({}^{\Gamma}_{b}m_1, {}^{\Gamma}_{b}m_2\right)}}, \tag{28}$$

where ${}^{\Gamma}_{b}m_1$ and ${}^{\Gamma}_{b}m_2$ are new BPAs after ${}^{\Gamma}m_1$ and ${}^{\Gamma}m_2$ are modified by the base belief function. The detailed modification process is showed as follows:

$$\begin{cases} {}^{\Gamma}_{b}m_1(A_i) = \dfrac{{}^{\Gamma}m_1(A_i) + m_b(A_i)}{2}, \\ {}^{\Gamma}_{b}m_2(A_i) = \dfrac{{}^{\Gamma}m_2(A_i) + m_b(A_i)}{2}, \end{cases} \tag{29}$$

where $m_b(A_i) = 1/(2^N - 1)$.

The EBD is an improved BD by modifying BPA; in the same way as the BD, it can also be regarded as a belief divergence of the IQ(m). In addition, the EBD maintains the excellent qualities of the BD, namely, it can differentiate multielement sets from singletons and allow for the correlation between subsets. Furthermore, the EBD improves the performance of the BD to measure the dissimilarity of evidence more effectively.

In order to show the calculation process clearly, Example 2 is adopted. The divergence measures among m_1, m_2, and m_3 are calculated by the EBD as follows.

In Example 2, as for m_1 and m_2, there are four focal elements $\{A\}$, $\{B\}$, $\{A, B\}$, and $\{A, C\}$ that satisfy $m_1(A_i) \neq 0 \vee m_2(A_i) \neq 0, A_i \in 2^\Theta$. According to the (27), it is obtained that β is 1. For convenient calculation, m_1 and m_2 are simplified as follows:

$$\begin{aligned} m_1&: (0.3, 0.4, 0.3, 0); \\ m_2&: (0.3, 0.4, 0, 0.3). \end{aligned} \tag{30}$$

In accordance to (18), the adjustment function Γ_{A_i,A_j} between m_1 and m_2 is obtained in the following Table 2.

From (20), modifying m_1 and m_2 by adjustment function, ${}^{\Gamma}m_1$ and ${}^{\Gamma}m_2$ are obtained as follows:

$$\begin{aligned} {}^{\Gamma}m_1&: (0.2353, 0.3553, 0.3258, 0.0837); \\ {}^{\Gamma}m_2&: (0.2477, 0.3000, 0.1890, 0.2632). \end{aligned} \tag{31}$$

Because $\Theta = \{A, B, C, D\}$ includes 4 mutually exclusive and collectively exhaustive events, according to (5), the base belief function $m_b = 1/(2^4 - 1) = 0.0667$. By (29), after ${}^{\Gamma}m_1$ and ${}^{\Gamma}m_2$ are averaged with m_b, ${}^{\Gamma}_{b}m_1$ and ${}^{\Gamma}_{b}m_2$ are obtained as follows:

$$\begin{aligned} {}^{\Gamma}_{b}m_1&: (0.1510, 0.2110, 0.1963, 0.0752); \\ {}^{\Gamma}_{b}m_2&: (0.1572, 0.1834, 0.1279, 0.1650). \end{aligned} \tag{32}$$

From (16), $\mathrm{BBC}({}^{\Gamma}_{b}m_1, {}^{\Gamma}_{b}m_2)$, $\mathrm{BBC}({}^{\Gamma}_{b}m_1, {}^{\Gamma}_{b}m_1)$, and $\mathrm{BBC}({}^{\Gamma}_{b}m_2, {}^{\Gamma}_{b}m_2)$ are gotten as follows:

$$\begin{aligned} \mathrm{BBC}\left({}^{\Gamma}_{b}m_1, {}^{\Gamma}_{b}m_2\right) &= 0.4407, \\ \mathrm{BBC}\left({}^{\Gamma}_{b}m_1, {}^{\Gamma}_{b}m_1\right) &= 0.4525, \\ \mathrm{BBC}\left({}^{\Gamma}_{b}m_2, {}^{\Gamma}_{b}m_2\right) &= 0.4382. \end{aligned} \tag{33}$$

Therefore, according to (28), we have

$$\mathrm{EBD}(m_1, m_2) = 1 \times \sqrt{1 - \frac{0.4407}{0.4525 + 0.4382 - 0.4407}} = 0.1438. \tag{34}$$

Similarly, $\mathrm{EBD}(m_1, m_3)$ and $\mathrm{EBD}(m_2, m_3)$ are calculated as follows:

$$\begin{aligned} \mathrm{EBD}(m_1, m_3) &= 0.2403, \\ \mathrm{EBD}(m_2, m_3) &= 0.1917. \end{aligned} \tag{35}$$

The result shows that $\mathrm{EBD}(m_1, m_2) = 0.1438 < \mathrm{EBD}(m_2, m_3) = 0.1917 < \mathrm{EBD}(m_1, m_3) = 0.2403$. It is more reasonable than the original results generated by BH divergence.

Besides, for the purpose of verifying whether the EBD have solved Case 11 and Case 12, the two cases are recalculated by the EBD and the results are compared with the BD in Table 3.

From Table 3, in Case 11, the conflict degree of group 2 by the EBD is smaller than that of group 1, in Case 12, with the uncertainty of the three groups of evidence increasing, the EBD is diminishing, which conforms to the analysis of the two cases. Consequently, the EBD is more reasonable and valid than the BD for evidence discrepancy measurement.

4.4. The Properties of the Enhanced Belief Divergence. In this section, the major properties of the enhanced belief divergence EBD are presented as follows.

Table 2: The adjustment function Γ_{A_i,A_j} between m_1 and m_2.

Γ_{A_i,A_j}	A	B	AB	AC
A	3/5	0	1/5	1/5
B	0	3/4	1/4	0
AB	7/38	7/38	21/38	3/38
AC	7/31	0	3/31	21/31

Table 3: The results comparison with the BD in Case 11 and Case 12.

Case	BD	EBD
Case 11	$\mathrm{BD}(m_1,m_2)=1$ $\mathrm{BD}(m_3,m_4)=1$	$\mathrm{EBD}(m_1,m_2)=0.7930$ $\mathrm{EBD}(m_3,m_4)=0.7732$
Case 12	$\mathrm{BD}(m_1,m_2)=0.7559$ $\mathrm{BD}(m_3,m_4)=0.7559$ $\mathrm{BD}(m_5,m_6)=0.7559$	$\mathrm{EBD}(m_1,m_2)=0.7337$ $\mathrm{EBD}(m_3,m_4)=0.3669$ $\mathrm{EBD}(m_5,m_6)=0.2446$

Theorem 15. *The EBD has the properties of boundedness, nondegeneracy, and symmetry.*

Property 16. Let m_1 and m_2 be two BPAs defined on the frame of discernment Θ:

(1) Boundedness: $0 \le \mathrm{EBD}(m_1,m_2) \le 1$;

(2) Nondegeneracy: $\mathrm{EBD}(m_1,m_2)=0$ if and only if $m_1=m_2$;

(3) Symmetry: $\mathrm{EBD}(m_1,m_2)=\mathrm{EBD}(m_2,m_1)$.

Proof. (1) m_1 and m_2 satisfy $0 \le m_1(A_i), m_2(A_i) \le 1$. In the light of the characteristics of the adjustment function and base belief function, ${}^{\Gamma}_{b}m_1$ and ${}^{\Gamma}_{b}m_2$ meet with $0 \le {}^{\Gamma}_{b}m_1(A_i), {}^{\Gamma}_{b}m_2(A_i) \le 1$. According to the mean inequality, we have ${}^{\Gamma}_{b}m_1(A_i) + {}^{\Gamma}_{b}m_2(A_i) \ge 2\sqrt{{}^{\Gamma}_{b}m_1(A_i){}^{\Gamma}_{b}m_2(A_i)}$, therefore,

$$\sum_{i=1}^{n}\frac{{}^{\Gamma}_{b}m_1(A_i)}{2^{|A_i|}-1}+\sum_{i=1}^{n}\frac{{}^{\Gamma}_{b}m_2(A_i)}{2^{|A_i|}-1}=\sum_{i=1}^{n}\frac{{}^{\Gamma}_{b}m_1(A_i)+{}^{\Gamma}_{b}m_2(A_i)}{2^{|A_i|}-1}\ge\sum_{i=1}^{n}\frac{\sqrt{{}^{\Gamma}_{b}m_1(A_i){}^{\Gamma}_{b}m_2(A_i)}}{2^{|A_i|}-1}. \tag{36}$$

Then, we obtain

$$\frac{\sum_{i=1}^{n}\sqrt{{}^{\Gamma}_{b}m_1(A_i){}^{\Gamma}_{b}m_2(A_i)}/\left(2^{|A_i|}-1\right)}{\sum_{i=1}^{n}{}^{\Gamma}_{b}m_1(A_i)/\left(2^{|A_i|}-1\right)+\sum_{i=1}^{n}{}^{\Gamma}_{b}m_2(A_i)/\left(2^{|A_i|}-1\right)-\sum_{i=1}^{n}\sqrt{{}^{\Gamma}_{b}m_1(A_i){}^{\Gamma}_{b}m_2(A_i)}/\left(2^{|A_i|}-1\right)}\ge 0. \tag{37}$$

According to

$$\sum_{i=1}^{n}\frac{{}^{\Gamma}_{b}m_1(A_i)}{2^{|A_i|}-1}+\sum_{i=1}^{n}\frac{{}^{\Gamma}_{b}m_2(A_i)}{2^{|A_i|}-1}\ge\sum_{i=1}^{n}\frac{2\sqrt{{}^{\Gamma}_{b}m_1(A_i){}^{\Gamma}_{b}m_2(A_i)}}{2^{|A_i|}-1}, \tag{38}$$

we have

$$\sum_{i=1}^{n}\frac{{}^{\Gamma}_{b}m_1(A_i)}{2^{|A_i|}-1}+\sum_{i=1}^{n}\frac{{}^{\Gamma}_{b}m_2(A_i)}{2^{|A_i|}-1}-\sum_{i=1}^{n}\frac{\sqrt{{}^{\Gamma}_{b}m_1(A_i){}^{\Gamma}_{b}m_2(A_i)}}{2^{|A_i|}-1}\ge\sum_{i=1}^{n}\frac{\sqrt{{}^{\Gamma}_{b}m_1(A_i){}^{\Gamma}_{b}m_2(A_i)}}{2^{|A_i|}-1}. \tag{39}$$

Therefore,

$$\frac{\sum_{i=1}^{n}\sqrt{{}_b^{\Gamma}m_1(A_i)\,{}_b^{\Gamma}m_2(A_i)}/\left(2^{|A_i|}-1\right)}{\sum_{i=1}^{n}{}_b^{\Gamma}m_1(A_i)/\left(2^{|A_i|}-1\right)+\sum_{i=1}^{n}{}_b^{\Gamma}m_2(A_i)/\left(2^{|A_i|}-1\right)-\sum_{i=1}^{n}\sqrt{{}_b^{\Gamma}m_1(A_i)\,{}_b^{\Gamma}m_2(A_i)}/\left(2^{|A_i|}-1\right)}\leq 1. \tag{40}$$

As a result,

$$0\leq\frac{\sum_{i=1}^{n}\sqrt{{}_b^{\Gamma}m_1(A_i)\,{}_b^{\Gamma}m_2(A_i)}/\left(2^{|A_i|}-1\right)}{\sum_{i=1}^{n}{}_b^{\Gamma}m_1(A_i)/\left(2^{|A_i|}-1\right)+\sum_{i=1}^{n}{}_b^{\Gamma}m_2(A_i)/\left(2^{|A_i|}-1\right)-\sum_{i=1}^{n}\sqrt{{}_b^{\Gamma}m_1(A_i)\,{}_b^{\Gamma}m_2(A_i)}/\left(2^{|A_i|}-1\right)}\leq 1. \tag{41}$$

Finally,

$$0\leq \mathrm{EBD}(m_1,m_2)=\sqrt{1-\frac{\sum_{i=1}^{n}\sqrt{{}_b^{\Gamma}m_1(A_i)\,{}_b^{\Gamma}m_2(A_i)}/\left(2^{|A_i|}-1\right)}{\sum_{i=1}^{n}{}_b^{\Gamma}m_1(A_i)/\left(2^{|A_i|}-1\right)+\sum_{i=1}^{n}{}_b^{\Gamma}m_2(A_i)/\left(2^{|A_i|}-1\right)-\sum_{i=1}^{n}\sqrt{{}_b^{\Gamma}m_1(A_i)\,{}_b^{\Gamma}m_2(A_i)}/\left(2^{|A_i|}-1\right)}}\leq 1. \tag{42}$$

The boundedness has been proven. □

Proof. (2) Given two BPAs m_1 and m_2 defined on Θ:

$$\begin{aligned}
&m_1=m_2\Rightarrow {}^{\Gamma}m_1(A_i)={}^{\Gamma}m_2(A_i)\Rightarrow {}_b^{\Gamma}m_1(A_i)={}_b^{\Gamma}m_2(A_i)\\
&\Rightarrow\sum_{i=1}^{n}\frac{{}_b^{\Gamma}m_1(A_i)}{2^{|A_i|}-1}=\sum_{i=1}^{n}\frac{{}_b^{\Gamma}m_2(A_i)}{2^{|A_i|}-1}=\sum_{i=1}^{n}\frac{\sqrt{{}_b^{\Gamma}m_1(A_i)\,{}_b^{\Gamma}m_2(A_i)}}{2^{|A_i|}-1}\\
&\Rightarrow\frac{\sum_{i=1}^{n}\sqrt{{}_b^{\Gamma}m_1(A_i)\,{}_b^{\Gamma}m_2(A_i)}/\left(2^{|A_i|}-1\right)}{\sum_{i=1}^{n}{}_b^{\Gamma}m_1(A_i)/\left(2^{|A_i|}-1\right)+\sum_{i=1}^{n}{}_b^{\Gamma}m_2(A_i)/\left(2^{|A_i|}-1\right)-\sum_{i=1}^{n}\sqrt{{}_b^{\Gamma}m_1(A_i)\,{}_b^{\Gamma}m_2(A_i)}/\left(2^{|A_i|}-1\right)}=1\\
&\Rightarrow\mathrm{EBD}(m_1,m_2)=\sqrt{1-\frac{\sum_{i=1}^{n}\sqrt{{}_b^{\Gamma}m_1(A_i)\,{}_b^{\Gamma}m_2(A_i)}/\left(2^{|A_i|}-1\right)}{\sum_{i=1}^{n}{}_b^{\Gamma}m_1(A_i)/\left(2^{|A_i|}-1\right)+\sum_{i=1}^{n}{}_b^{\Gamma}m_2(A_i)/\left(2^{|A_i|}-1\right)-\sum_{i=1}^{n}\sqrt{{}_b^{\Gamma}m_1(A_i)\,{}_b^{\Gamma}m_2(A_i)}/\left(2^{|A_i|}-1\right)}}=0.
\end{aligned} \tag{43}$$

Conversely,

$$\begin{aligned}
&\mathrm{EBD}(m_1,m_2)=\sqrt{1-\frac{\sum_{i=1}^{n}\sqrt{{}_b^{\Gamma}m_1(A_i)\,{}_b^{\Gamma}m_2(A_i)}/\left(2^{|A_i|}-1\right)}{\sum_{i=1}^{n}{}_b^{\Gamma}m_1(A_i)/\left(2^{|A_i|}-1\right)+\sum_{i=1}^{n}{}_b^{\Gamma}m_2(A_i)/\left(2^{|A_i|}-1\right)-\sum_{i=1}^{n}\sqrt{{}_b^{\Gamma}m_1(A_i)\,{}_b^{\Gamma}m_2(A_i)}/\left(2^{|A_i|}-1\right)}}=0\\
&\Rightarrow\frac{\sum_{i=1}^{n}\sqrt{{}_b^{\Gamma}m_1(A_i)\,{}_b^{\Gamma}m_2(A_i)}/\left(2^{|A_i|}-1\right)}{\sum_{i=1}^{n}{}_b^{\Gamma}m_1(A_i)/\left(2^{|A_i|}-1\right)+\sum_{i=1}^{n}{}_b^{\Gamma}m_2(A_i)/\left(2^{|A_i|}-1\right)-\sum_{i=1}^{n}\sqrt{{}_b^{\Gamma}m_1(A_i)\,{}_b^{\Gamma}m_2(A_i)}/\left(2^{|A_i|}-1\right)}=1\\
&\Rightarrow\sum_{i=1}^{n}\frac{{}_b^{\Gamma}m_1(A_i)}{2^{|A_i|}-1}+\sum_{i=1}^{n}\frac{{}_b^{\Gamma}m_2(A_i)}{2^{|A_i|}-1}=2\sum_{i=1}^{n}\frac{\sqrt{{}_b^{\Gamma}m_1(A_i)\,{}_b^{\Gamma}m_2(A_i)}}{2^{|A_i|}-1}\\
&\Rightarrow\sum_{i=1}^{n}\frac{{}_b^{\Gamma}m_1(A_i)+{}_b^{\Gamma}m_2(A_i)-2\sqrt{{}_b^{\Gamma}m_1(A_i)\,{}_b^{\Gamma}m_2(A_i)}}{2^{|A_i|}-1}=0\\
&\Rightarrow{}_b^{\Gamma}m_1(A_i)+{}_b^{\Gamma}m_2(A_i)=2\sqrt{{}_b^{\Gamma}m_1(A_i)\,{}_b^{\Gamma}m_2(A_i)}\\
&\Rightarrow{}_b^{\Gamma}m_1(A_i)={}_b^{\Gamma}m_2(A_i)\\
&\Rightarrow{}^{\Gamma}m_1(A_i)={}^{\Gamma}m_2(A_i)\\
&\Rightarrow m_1=m_2.
\end{aligned}\tag{44}$$

The nondegeneracy has been proven. □

Proof. (3) Given two BPAs m_1 and m_2 defined on Θ:

$$\begin{aligned}
&\mathrm{EBD}(m_1,m_2)=\sqrt{1-\frac{\sum_{i=1}^{n}\sqrt{{}_b^{\Gamma}m_1(A_i)\,{}_b^{\Gamma}m_2(A_i)}/\left(2^{|A_i|}-1\right)}{\sum_{i=1}^{n}{}_b^{\Gamma}m_1(A_i)/\left(2^{|A_i|}-1\right)+\sum_{i=1}^{n}{}_b^{\Gamma}m_2(A_i)/\left(2^{|A_i|}-1\right)-\sum_{i=1}^{n}\sqrt{{}_b^{\Gamma}m_1(A_i)\,{}_b^{\Gamma}m_2(A_i)}/\left(2^{|A_i|}-1\right)}},\\
&\mathrm{EBD}(m_2,m_1)=\sqrt{1-\frac{\sum_{i=1}^{n}\sqrt{{}_b^{\Gamma}m_2(A_i)\,{}_b^{\Gamma}m_1(A_i)}/\left(2^{|A_i|}-1\right)}{\sum_{i=1}^{n}{}_b^{\Gamma}m_2(A_i)/\left(2^{|A_i|}-1\right)+\sum_{i=1}^{n}{}_b^{\Gamma}m_1(A_i)/\left(2^{|A_i|}-1\right)-\sum_{i=1}^{n}\sqrt{{}_b^{\Gamma}m_2(A_i)\,{}_b^{\Gamma}m_1(A_i)}/\left(2^{|A_i|}-1\right)}}.
\end{aligned}\tag{45}$$

Apparently,

$$\mathrm{EBD}(m_1,m_2)=\mathrm{EBD}(m_2,m_1).\tag{46}$$

The symmetry has been proven. □

4.5. The Comparison Analysis. In this section, several comparative examples with Florea and Bossé's distance $d_B(p=1/2)$, BJS divergence, and BH distance are utilized to illustrate the validity and superiority of the EBD.

Example 4. Suppose m_1 and m_2 are two independent BPAs defined on $\Theta=\{A,B,C,D,E,F,G,H,I,J\}$. A_t is a variable set from $\{A\}$ to Θ, t: $1\longrightarrow 10$, adding one element to the set each time, in the order from A to J.

$$\begin{aligned}
&m_1\colon m_1(\{B\})=0.05, m_1(\{A_t\})=0.95;\\
&m_2\colon m_2(\{B\})=0.95, m_2(\{A_t\})=0.05.
\end{aligned}\tag{47}$$

In this example, the enhancement factor β of the EBD is 1. As $t=1$, it is discovered that m_1 and m_2, respectively, support $\{A\}$ and $\{B\}$, which is highly conflicting. As $t=2$, A_t has the element B, it increases the probable belief of $\{B\}$ in m_1, the discrepancy between m_1 and m_2 decreases. Then, as the number of elements in A_t enlarges, the divergence between m_1 and m_2 also enlarges.

However, as depicted in Figure 2(a), it is clear that Florea and Bossé's distance d_B and BJS divergence keep unchanged, which is not proper. In addition, although BH distance has varying values with t, it is unreasonable to have a downward trend. We can observe that only the EBD accords with the changing tendency of conflict degree between m_1 and m_2.

Example 5. Suppose m_1 and m_2 are two independent BPAs defined on $\Theta=\{A,B,C,D,E,F,G,H,I,J\}$, A_t is a variable set from $\{A\}$ to Θ, t: $1\longrightarrow 10$, the specific variations of A_t are the same as those in Example 4.

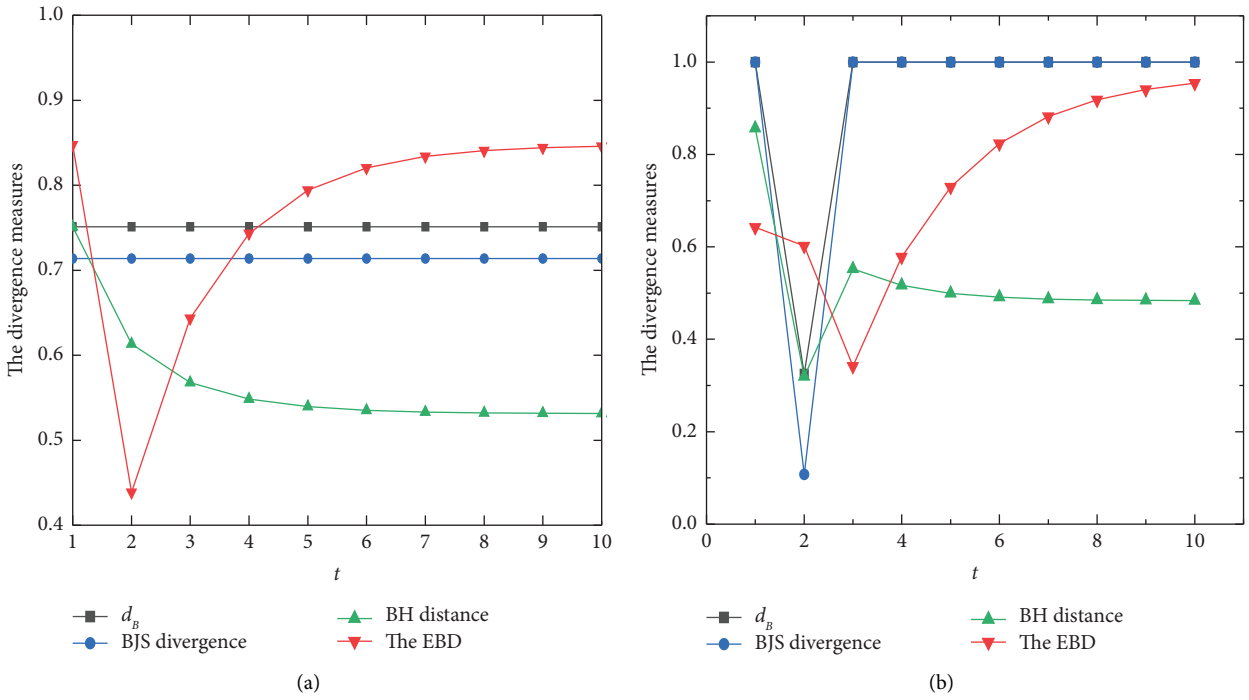

Figure 2: The comparison with the d_B, BJS divergence, and BH distance in Examples 4 and 5, (a) Example 4, (b) Example 5.

$$\begin{aligned} m_1\colon\ & m_1(\{A_t\}) = 1; \\ m_2\colon\ & m_2(\{A, B\}) = 0.8, \\ & m_2(\{C\}) = 0.2. \end{aligned} \tag{48}$$

In this example, m_1 has the varying focal elements $\{A_t\}$ and m_2 has the focal elements $\{A, B\}$ and $\{C\}$. Because the cardinality of them is not identical, the enhancement factor is 1. When $t = 1$, m_1 supports the $\{A\}$ and m_2 supports the $\{A, B\}$. As $t = 2$, m_1 completely supports the proposition $\{A, B\}$ same as the supportive proposition of m_2, thus, the value of divergence between m_1 and m_2 decreases. As $t = 3$, with the hypothesis C added to the $\{A_t\}$, m_1 has the possibility to support $\{C\}$, the conflict degree between m_1 and m_2 decreases. When $\{A_t\}$ continue to add other elements, the divergence is getting large.

As displayed in Figure 2(b), d_B and BJS divergence are always kept as one except $t = 2$. BH distance keeps decreasing with t in general. Obviously, it infers that the EBD can perform better than the other divergences on discrepancy measurement.

Example 6. Suppose m_1 and m_2 are two independent BPAs defined on Θ, A_t is a variable set defined as Table 4.

$$\begin{aligned} m_1\colon\ & m_1(\{A\}) = 0.7, m_1(\{A_t\}) = 0.3; \\ m_2\colon\ & m_2(\{A\}) = 0.7, m_2(\{A, B\}) = 0.3. \end{aligned} \tag{49}$$

In this example, the belief value distributions of m_1 and m_2 are identical, the difference between m_1 and m_2 is that between focal elements A_t and $\{A, B\}$. When $t = 1$, the two evidence is identical, so the evidence between m_1 and m_2 is 0. When $t = 2$, A_t in m_1 becomes $\{A, C\}$, which is different from $\{A, B\}$ in m_2. In the similar way, as $t = 3, 4$, it is just the hypothesis C that respectively changes to D and E, therefore, the divergence between m_1 and m_2 at $t = 2, 3, 4$ is the same. As $t = 5$, A_t in m_1 is $\{B, C\}$, the intersection of $\{A\}$ and A_t is $\varnothing$, which decreases the possibility to support $\{A\}$, so the value of divergence is much larger than the former states. The situation of $t = 6, 7$ is similar to that of $t = 5$, namely, m_1 and m_2 at $t = 5, 6, 7$ is also the same. The remaining circumstance $t = 8, 9, 10$ can be concluded likewise.

However, as portrayed in Figure 3, it can be observed that d_B, BJS divergence and BH distance maintain unchanged except at $t = 1$, which cannot reflect the correlation between different types of subsets. Therefore, the results by the EBD show more reasonable and effective.

5. A New EBD-Based Multisource Information Fusion Method

Multisource information fusion refers to the means that integrate data from various sensors to generate a rational and precise result. The data gathered from every sensor can be modeled as a piece of evidence, but the credibility of the evidence is susceptible to sensor failure or detrimental environmental factors, which have an impact on the accuracy of the result. Therefore, it is crucial to evaluate the reliability of evidence during the information fusion process.

In this section, based on the EBD and Deng entropy, a new multisource information fusion approach is devised. Specifically, the weight of evidence is decided by the divergence between the evidence and the uncertainty contained in evidence. The EBD can allude to the extent of evidence inconsistency, where the evidence modeled by the

Table 4: The variation of set A_t.

t	1	2	3	4	5	6	7	8	9	10
A_t	$\{A, B\}$	$\{A, C\}$	$\{A, D\}$	$\{A, E\}$	$\{B, C\}$	$\{B, D\}$	$\{B, E\}$	$\{C, D\}$	$\{C, E\}$	$\{D, E\}$

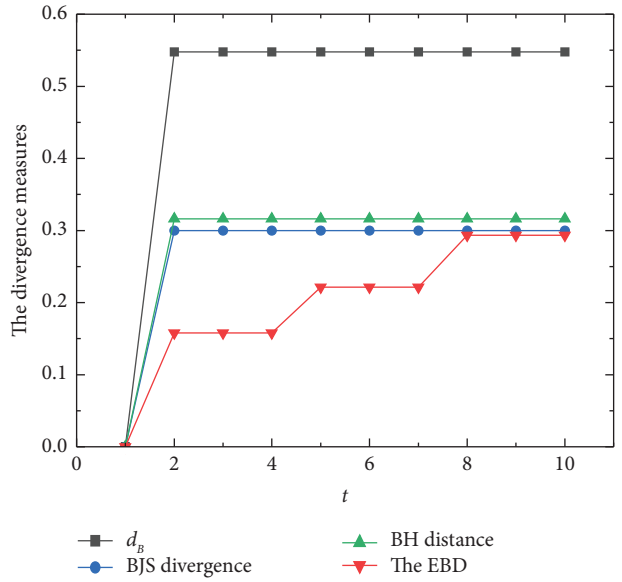

Figure 3: The comparison with the d_B, BJS divergence and BH distance in Example 6.

flawed information source is highly conflicting with the normal one. Deng entropy can be used to quantify the uncertainty of evidence, where the evidence with more uncertainty conserves a wealth of potential useful information. The algorithm flowchart of this method is shown in Figure 4 and the detailed steps are given as follows.

Assume that there are n sensors, from which n pieces of evidence $m_1, m_2, \ldots m_n$ are collected. The BPAs are defined on the frame of discernment $\Theta = \{A_1, A_2, \ldots, A_m\}$.

Step 1. Determining the credibility weight W_c of evidence.

Step 1.1: Construct divergence measure matrix.
Based on the EBD given in Equation (28), the divergence between evidence $m_i (i = 1, 2, \ldots, n)$ and $m_j (j = 1, 2, \ldots, n)$ is denoted as d_{ij}. Then, the divergence measure matrix $\mathrm{DMM} = (d_{ij})_{n\times n}$ can be established as follows:

$$\mathrm{DMM} = \begin{bmatrix} 0 & \cdots & d_{1i} & \cdots & d_{1n} \\ \vdots & \vdots & \vdots & \vdots & \vdots \\ d_{i1} & \cdots & 0 & \cdots & d_{in} \\ \vdots & \vdots & \vdots & \vdots & \vdots \\ d_{n1} & \cdots & d_{ni} & \cdots & 0 \end{bmatrix}. \tag{50}$$

Step 1.2: Calculate the average divergence measure.
On the basis of the DMM, the average divergence of evidence m_i is indicated as $\overline{d}(m_i)$, the formula is represented as follows:

$$\overline{d}(m_i) = \frac{\sum_{j=1}^{n} d_{ij}}{n-1}, \quad i = 1, \ldots, n; j = 1, \ldots, n. \tag{51}$$

Step 1.3: Generate the support degree.
The support degree $\mathrm{Sup}(m_i)$ of evidence m_i can be calculated as follows:

$$\mathrm{Sup}(m_i) = \frac{1}{\overline{d}(m_i)}, \quad i = 1, \ldots, n. \tag{52}$$

Step 1.4: Obtain the credibility weight.
The credibility weight $W_c(m_i)$ of evidence m_i can be obtained as follows:

$$W_c(m_i) = \frac{\mathrm{Sup}(m_i)}{\sum_{j=1}^{n} \mathrm{Sup}(m_j)}, \quad i = 1, \ldots, n. \tag{53}$$

Step 2. Forming the information volume weight W_{iv} of evidence.

Step 2.1: Calculate the Deng entropy.
According to equation (6), the Deng entropy $E_d(m_i)$ of evidence m_i is generated as follows:

$$E_d(m_i) = -\sum_{A\subseteq\Theta} m_i(A)\log_2 \frac{m_i(A)}{2^{|A|}-1}, \quad i = 1, \ldots, n. \tag{54}$$

Step 2.2: Get the information volume.
The information volume $\mathrm{IV}(m_i)$ of evidence m_i is defined as follows:

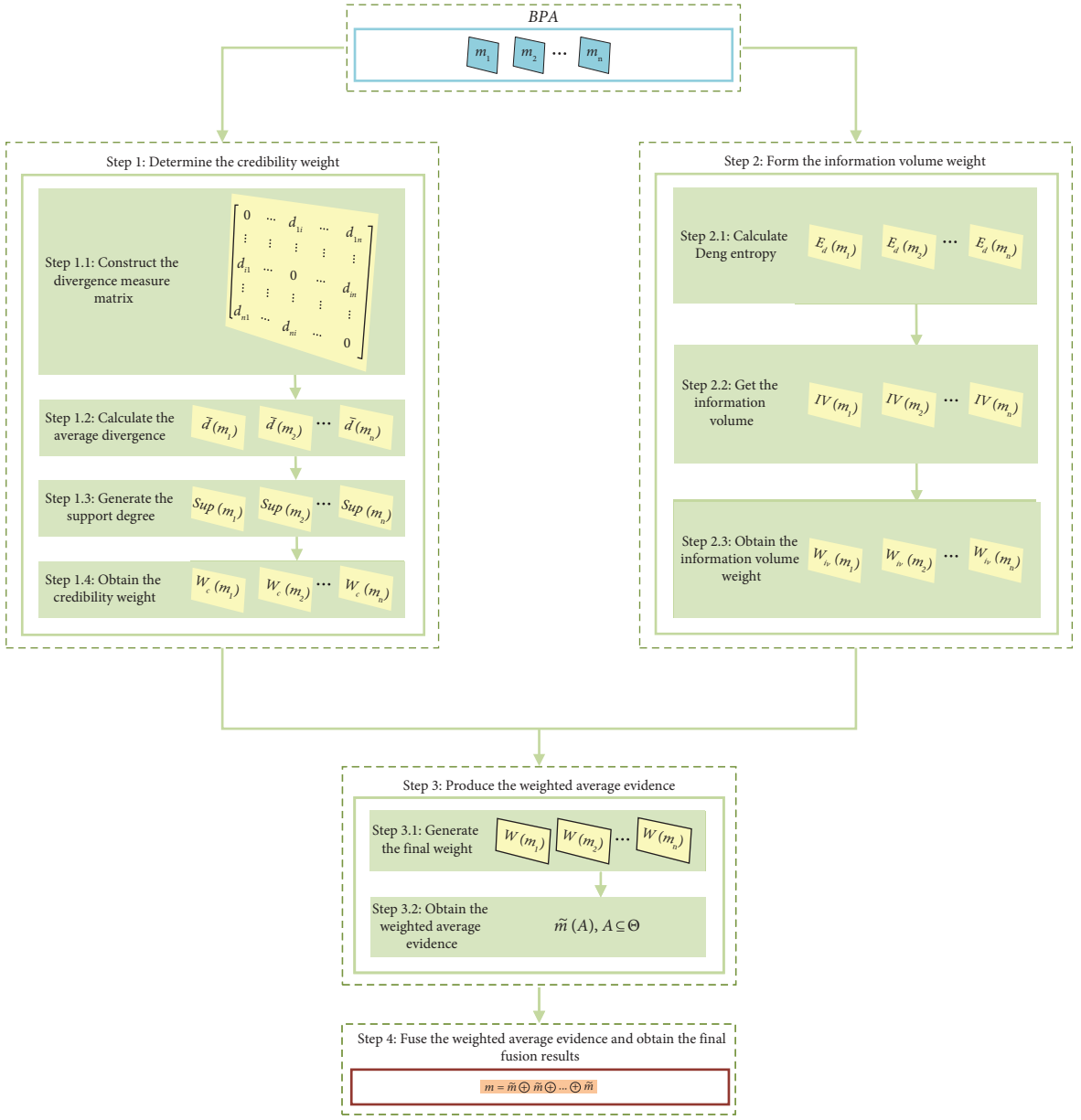

Figure 4: The flowchart of the EBD-based multisource information fusion algorithm.

$$\mathrm{IV}(m_i) = e^{E_d(m_i)}, \quad i = 1, \ldots, n. \tag{55}$$

Step 2.3: Obtain the information volume weight.
By normalizing the IV, the information volume weight $W_{iv}(m_i)$ of evidence m_i is denoted as follows:

$$W_{iv}(m_i) = \frac{\mathrm{IV}(m_i)}{\sum_{j=1}^{n} \mathrm{IV}(m_j)}, \quad i = 1, \ldots, n. \tag{56}$$

Step 3. Producing the weighted average evidence.

Step 3.1: Generate the final weight.
Combing the credibility weight and information volume weight of evidence m_i, the final weight $W(m_i)$ of evidence m_i is acquired as follows:

$$W(m_i) = \frac{W_c(m_i) \times W_{iv}(m_i)}{\sum_{i=1}^{n} W_c(m_i) \times W_{iv}(m_i)}, \quad i = 1, \ldots, n. \tag{57}$$

Step 3.2: Weight the body of evidence.
The weighted average evidence is calculated as follows:

$$\tilde{m}(A) = \sum_{i=1}^{n} W(m_i) \times m_i(A), A \subseteq \Theta. \tag{58}$$

Step 4. Fuse the weighted average evidence.

The weighted average evidence is fused with the Dempster's combination rule equation (4) by $n-1$ times, the eventual result is obtained as follows:

$$m = \underbrace{\widetilde{m} \oplus \widetilde{m} \oplus \cdots \oplus \widetilde{m}}_{n-1 \text{ times}}. \tag{59}$$

6. Experiment

To demonstrate the feasibility and effectiveness of our method, two experiments, i.e., a target recognition problem and a classification problem are presented. The comparison with other methods is conducted to further illustrate the superiority of the EBD-based multisource information fusion approach.

6.1. Target Recognition. In a multisensor-based target recognition system, suppose the frame of discernment, including three possible targets, is $\Theta = \{A, B, C\}$, there are five installed sensors $\{S_1, S_2, S_3, S_4, S_5\}$ in the system. The data collected from the five sensors are modeled as five BPAs, $\{m_1, m_2, m_3, m_4, m_5\}$, shown in Figure 5. This experimental data is based on Deng [33].

From Figure 5, it is noted that the target directivity of sensors m_1, m_3, m_4, and m_5 is more oriented to A; therefore, we can infer that A is the real target, which should be allocated a high level of accuracy in the fusion results. While only m_2 assigns most of its belief to strongly support the target B, it has a different direction from the other sensors. As a result, it is believed that m_2 is highly conflicting with other four pieces of evidence. As a comparison, the fusion results of the well-known methods and the proposed method are presented in Table 5.

As can be seen in Table 5, the comparative results indicate that A is the real target, which verifies the perception from the above analysis. Obtained by Dempster's method, the fusion result realizes C as the identified target and distributes zero belief to A. Evidently, such a result is unreasonable. Hence, it is unsuitable to adopt Dempster's combination rule directly to combine the conflicting evidence. Murphy's method can correctly determine the target type as A. Moreover, the recognized target of Deng's method is in accordance with that of Murphy's method with a higher belief. Although the two aforesaid methods are able to identify the real target, it is noteworthy that the proposed method can achieve the highest accuracy of 0.9904. From these findings, the proposed method can make a more accurate decision result when dealing with conflicting evidence.

6.2. Iris Classification. An iris dataset-based classification experiment, containing the data without conflict and with conflict, is implemented here. For the sake of fairly comparing the results, the generated BPAs in Qian [50] are referred to further assess the performance of our method.

6.2.1. Fusion without Conflict. There are three types of iris flowers (*Setosa*, *Versicolor*, and *Virginica*), and the framework of discernment is $\Theta = \{\text{Se}, \text{Vc}, \text{Vi}\}$. In addition, each type of iris flower has four attributes, namely *Sepal Length* (*SL*), *Sepal Width* (*SW*), *Petal Length* (*PL*), and *Petal Width* (*PW*). The converted BPAs based on the iris dataset are shown in Figure 6.

From Figure 6, the BPAs of the four attributes, m_1, m_2, m_3, and m_4, all bestow a relatively high belief to the flower type Se. In other words, there is no conflict between them, and the belief allocated to {Se} should be the highest after fusion. The fusion results of the proposed method and comparative methods are presented in Table 6. From Table 6, as we expected, all methods, including our method, can identify the flower type, when evidence is not conflicting.

6.2.2. Fusion with Conflict. To further verify the robustness of the proposed method, the data of attribute *SW* source is revised to serve as noisy evidence. A group of obtained evidence with conflict is shown in Figure 7. From Figure 7, it infers that the *SL* attribute has no clear directivity toward the flower types of *Se* and *Vc*, with proximate belief values of 0.3337 and 0.3165. While the *SW* attribute assigns almost all beliefs to *Vc*. The attributes of *PL* and *PW* believe that the test sample belongs to the flower type of *Se*. As a consequence, it is suggested that the correct flower type of the test sample is *Se*.

After conducting the proposed method and other researchers' schemes, the fusion results are shown in Table 7. As can be seen from Table 7, Dempster's method and Murphy's method trust that *Vc* is the real flower type of the test sample, and they give *Se* a low support degree, which yields a completely misleading result. Therefore, they cannot work effectively when the evidence is conflicting. Both Deng's method and the proposed method can precisely recognize the real target; what's more, the proposed method endows a larger belief to *Se* than Deng's method dose.

The reason why the proposed method outperforms other methods is that in Dempster's method, it directly uses the combination rule to fuse highly conflicting evidence, but produces a counter-intuitive result. To a certain extent, Murphy's method can handle the conflict by simply averaging the evidence. However, it makes all evidence have the same weight, which may eliminate the conflict among evidence and greatly influence the fusion result. Taking the distance between evidence into account, Deng's method distributes different weights to evidence, while it ignores the information volume of evidence itself. The proposed method considers not only the divergence but also the information volume to thoroughly calculate the weight of the evidence. Therefore, it can be concluded that the proposed method has a preferable effect on decision fusion.

7. Application in Failure Mode and Effects Analysis of Aircraft Turbine Rotor Blades

Information fusion is widely applied in risk evaluation and expert system [51, 52]. In the aerospace field, rotor blades, including compressor rotor blades and turbo rotor blades, are the major components of an aircraft turbine, whose reliability seriously affects the overall aircraft turbine security. In order to enhance their safety, failure mode and effects analysis (FMEA) can facilitate the identification of potential failures

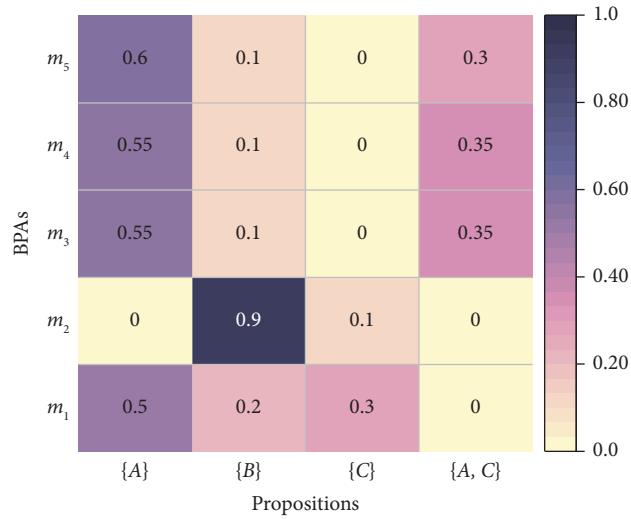

Figure 5: The five BPAs from sensors in target recognition.

Table 5: The fusion results of the four methods in target recognition.

Methods	$m(\{A\})$	$m(\{B\})$	$m(\{C\})$	$m(\{A, C\})$	Target
Dempster [5]	0	0.1404	0.8596	0	C
Murphy [20]	0.9688	0.0156	0.0127	0.0029	A
Deng [33]	0.9869	0.0010	0.0088	0.0032	A
Proposed method	0.9904	0.0001	0.0047	0.0047	A

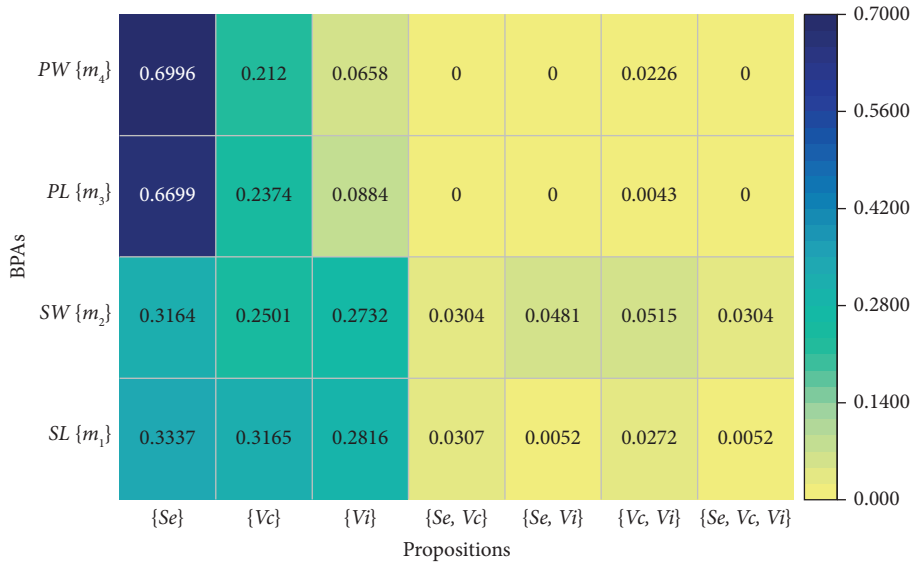

Figure 6: The BPAs from four attributes without conflict in the iris classification.

and determine the effect of each failure to decrease failure rates and avoid hazardous accidents. However, there may be a load of failure modes with different risks and effects. Consequently, it is necessary to prioritize their risks. The risk priority number (RPN) is one way to rank these failure modes. The RPN is the product of the three factors, the probability of the occurrence of a failure mode (O), the severity of a failure effect (S), and the probability of a failure being detected (D), expressed as RPN = $O \times S \times D$. However, multiple experts may give different risk evaluations on three risk factors for one failure mode, which may be imprecise and uncertain. Therefore, multisource information fusion can be used to promote the accuracy of evaluation.

In this section, the EBD-based multisource fusion method is adopted to calculate the new mean value of the RPN, and then determine the risk priority of multiple failure modes of aircraft turbine rotor blades, in which the EBD plays a key role in deciding the weights of experts. Furthermore, the risk ranking results are compared with other methods to determine the validity of our method.

Table 6: The fusion results of non-conflict data by different methods in iris classification.

Method	$m(\{Se\})$	$m(\{Vc\})$	$m(\{Vi\})$	$m(\{Se, Vc\})$	$m(\{Se, Vi\})$	$m(\{Vc, Vi\})$	$m(\{Se, Vc, Vi\})$
Dempster [5]	0.8940	0.0933	0.0127	0	0	0	0
Murphy [20]	0.8854	0.0880	0.0266	0	0	0	0
Deng [33]	0.8867	0.0872	0.0261	0	0	0	0
Proposed method	0.7230	0.1707	0.1061	0	0	0	0

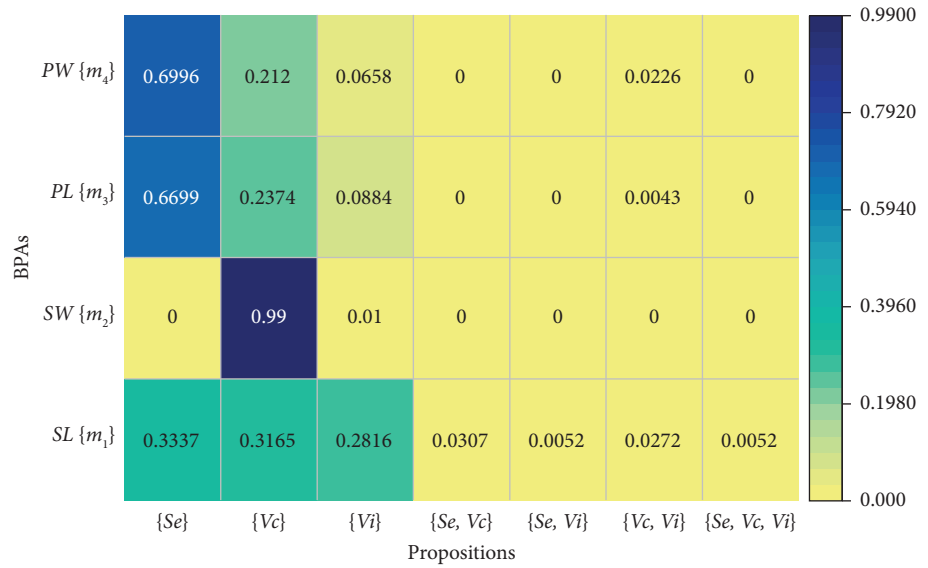

Figure 7: The BPAs from four attributes with conflict in the iris classification.

Table 7: The fusion results of conflict data by different methods in iris classification.

Method	$m(\{Se\})$	$m(\{Vc\})$	$m(\{Vi\})$	$m(\{Se, Vc\})$	$m(\{Se, Vi\})$	$m(\{Vc, Vi\})$	$m(\{Se, Vc, Vi\})$
Dempster [5]	0	0.9988	0.0012	0	0	0	0
Murphy [20]	0.4422	0.5546	0.0032	0	0	0	0
Deng [33]	0.7301	0.2652	0.0047	0	0	0	0
Proposed method	0.8322	0.1511	0.0167	0	0	0	0

7.1. Problem Statement. In FMEA, there are three risk factors: occurrence (O), severity (S) and detection (D) included in the RPN, which have a numeric scale rating from 1 to 10, suggested criteria of rating for each risk factor is listed as Tables S1–S3 in Supplementary Description. Suppose there are J experts: $\{E_1, \ldots, E_J\}$ and N failure modes: $\{FM_1, \ldots, FM_N\}$. The experts may give their different evaluations to the same risk factor, which are modeled as J evidence: $\{m_1, \ldots, m_J\}$. Consequently, there are three discernment frames respectively for O, S and D. Moreover, for the N failure modes, the total number of discernment frame is $3N$. Under this circumstance, the frame of discernment of the i th risk factor of the n th failure mode can be presented as follows:

$$\Theta_i^n = \{1, 2, 3, 4, 5, 6, 7, 8, 9, 10\}, \quad i = O, S, D; n = 1, 2, \ldots, N. \tag{60}$$

For convenience, Yang et al. simplified the frame of discernment Θ_i^n, which is denoted as follows [53]:

$$\Theta_i^n = \{\min X|_{X\subseteq\Theta_i^n}, \min X|_{X\subseteq\Theta_i^n} + 1, \ldots, \max X|_{X\subseteq\Theta_i^n}\}, \tag{61}$$

where $\min X|_{X\subseteq\Theta_i^n}$ and $\max X|_{X\subseteq\Theta_i^n}$ separately means the minimum and maximum of the rank of the n th failure mode to the i th risk factor from J experts.

7.2. Implementation. The rotor blades of an aircraft turbine consist of two subsystems, the compressor rotor blades and the turbo rotor blades. According to the practical engineering background, there are nine potential failure modes in the compressor rotor blades and eight failure modes in the turbo rotor blades, namely, 17 recognized failure modes $\{FM_1, \ldots, FM_{17}\}$ in total [53].

In this experiment, the BPAs in Yuan [54], transformed from the evaluation information of the three experts $\{E_1, E_2, E_3\}$ to O, S and D on the 17 failure modes, are referred. On the simplified frame of discernment in (61), we

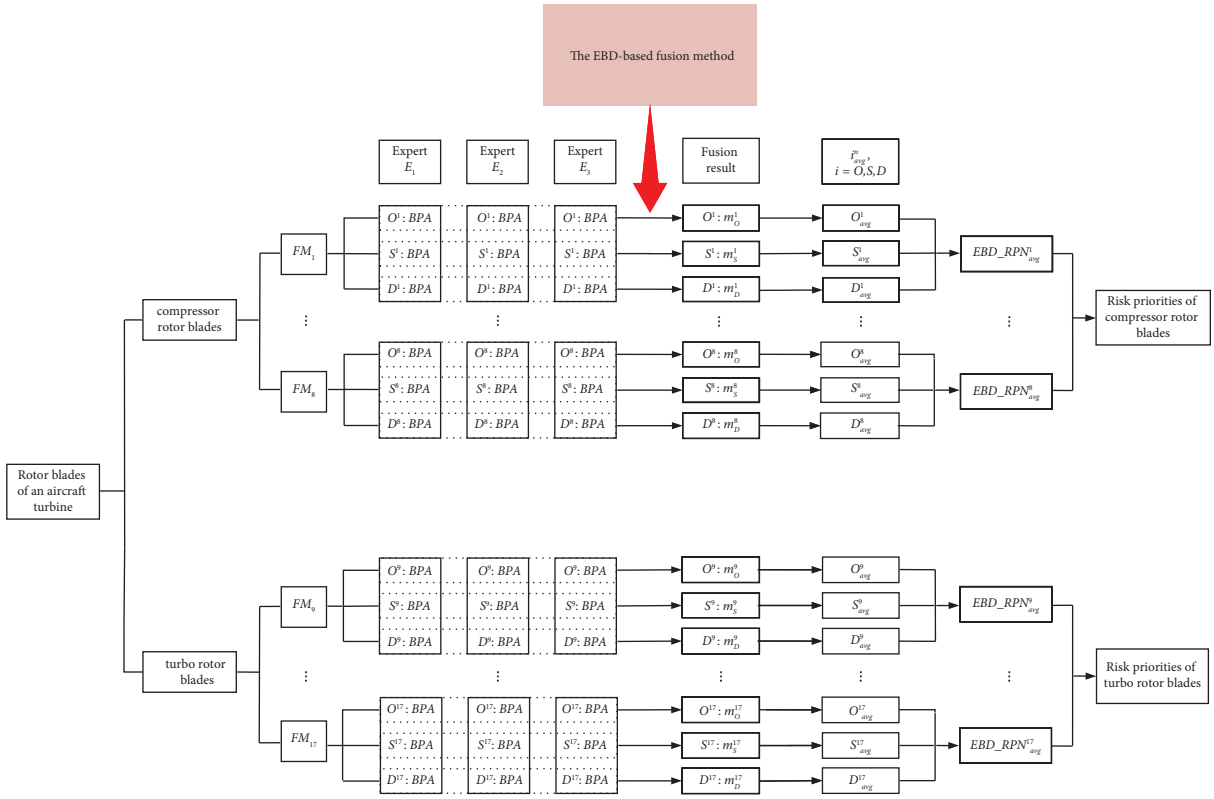

Figure 8: The flowchart for prioritizing risk based on the $\text{EBD\_RPN}_{\text{avg}}$.

use the EBD-based information fusion algorithm in Section 5 to aggregate the BPAs of i th risk factor in the n th failure mode, the fusion results are obtained as $m_i^n(A), A \subseteq \Theta_i^n$, $i = O, S, D$, where A represents the rating of the risk factors. Attributed to the axiom of additivity, $m_i^n(A)$ can be regarded as the probability of A. According to [54], the mean value of RPN can be used to compare the overall risk of each failure mode. Based on the proposed fusion method, the new mean value of RPN, named as $\text{EBD\_RPN}_{\text{avg}}$, can be obtained by

$$i^n_{\text{avg}} = \sum_{A=1}^{10} A \times m_i^n(A), \quad i = O,S,D; n = 1,2,\ldots,17,$$
$$\text{EBD\_RPN}^n_{\text{avg}} = O^n_{\text{avg}} \times S^n_{\text{avg}} \times D^n_{\text{avg}}. \tag{62}$$

For ease of understanding, the above process of calculating the $\text{EBD\_RPN}_{\text{avg}}$ is showed in the form of a flowchart as Figure 8. At the same time, the calculated $\text{EBD\_RPN}_{\text{avg}}s$ of 17 failure modes are presented in Table 8.

As shown in Table 8, among the 8 failure modes of compressor rotor blades, failure mode 2 has the largest $\text{EBD\_RPN}_{\text{avg}}$ and failure mode 5 has the least $\text{EBD\_RPN}_{\text{avg}}$. Decided by sorting numeric size of $\text{EBD\_RPN}_{\text{avg}}$, the risk priority order of them is $FM_2 \succ FM_6 \succ FM_1 \succ FM_3 \succ FM_7 \succ FM_4 \succ FM_8 \succ FM_5$. Among the 9 failure modes of turbo rotor blades, failure mode 9 has the largest $\text{EBD\_RPN}_{\text{avg}}$ and failure mode 16 has the least $\text{EBD\_RPN}_{\text{avg}}$, the risk priority order of them is $FM_9 \succ FM_{10} \succ FM_{14} \succ FM_{12} \succ FM_{11} \succ FM_{13} \succ FM_{15} \succ FM_{17} \succ FM_{16}$, $\succ$ hints that the previous item has a higher priority.

Several comparative methods to investigate the RPN in FMEA are introduced here. In detail, AMWRPN takes into consideration of the relative weight of different risk factors, by measuring the ambiguity degree of the experts' assessments, to get a new ambiguity measure weighted risk priority number [55]. MVRPN calculates the average of the obtained RPN values with the modified belief function and combination rule [53]. The improved MVRPN constructs the BPA to handle the conflicting evidence and refine the MVRPN [56]. The method in the literature [54] gives a new mean value of RPN based on triangular fuzzy numbers, negation of BPAs and evidence distance. The comparison results with the above methods are shown in Table 9.

From Table 9, the results of the AMWRPN method in $FM_1 - FM_{17}$ are very close. And the values of the MVRPN method are similar to those of the improved MVRPN method. In addition, for turbo rotor blades, in the MVRPN method, failure mode 10, 13, and 14 have the same RPN 60, and failure mode 11 and 12 have the same RPN 50. In the improved MVRPN method, the RPN of failure mode 11, 12, and 13 is all the same. Remarkably, the results by our method are very close to those of RPN_{avg}. It is worth noting that the values of $\text{EBD\_RPN}_{\text{avg}}$ are not dense and well distinguished, which contributes to the differentiated risk ranking of multiple failure modes of rotor blades.

Table 8: The EBD_RPN$_{avg}$s of 17 failure modes.

Component	Compressor rotor blades											Turbo rotor blades					
Failure mode	1	2	3	4	5	6	7	8	9	10	11	12	13	14	15	16	17
EBD_RPN$_{avg}$	46.0507	70.3001	34.9330	20.6688	3.9263	65.9171	24.5679	17.3751	81.5061	68.6229	57.3929	63.1752	56.8269	68.3174	46.2888	24.9738	32.9089

Table 9: The RPNs of 17 failure modes by different methods.

Component	Compressor rotor blades									Turbo rotor blades							
Failure mode	1	2	3	4	5	6	7	8	9	10	11	12	13	14	15	16	17
AMWRPN [55]	5.1551	5.3174	3.8684	3.3302	1.6529	5.0964	3.3567	3.2975	8.3797	5.0964	4.7399	5.0973	4.9447	5.4187	5.9509	3.7560	5.0554
MVRPN [53]	42.56	64.00	30.00	18.00	4.17	60.00	21.00	15.00	78.92	60.00	50.00	50.00	60.00	60.00	42.00	23.88	50.90
Improved MVRPN [56]	42.56	64.05	30.00	17.97	3.14	60.00	21.00	15.00	79.57	60.00	50.00	50.00	50.00	60.04	42.09	23.86	30.05
RPN_{avg} [54]	45.81	70.27	34.95	20.61	4.00	65.94	24.58	17.42	81.65	68.66	57.42	63.13	56.85	68.13	46.22	25.02	32.92
EBD_RPN_{avg}	46.0507	70.3001	34.9330	20.6688	3.9263	65.9171	24.5679	17.3751	81.5061	68.6229	57.3929	63.1752	56.8269	68.3174	46.2888	24.9738	32.9089

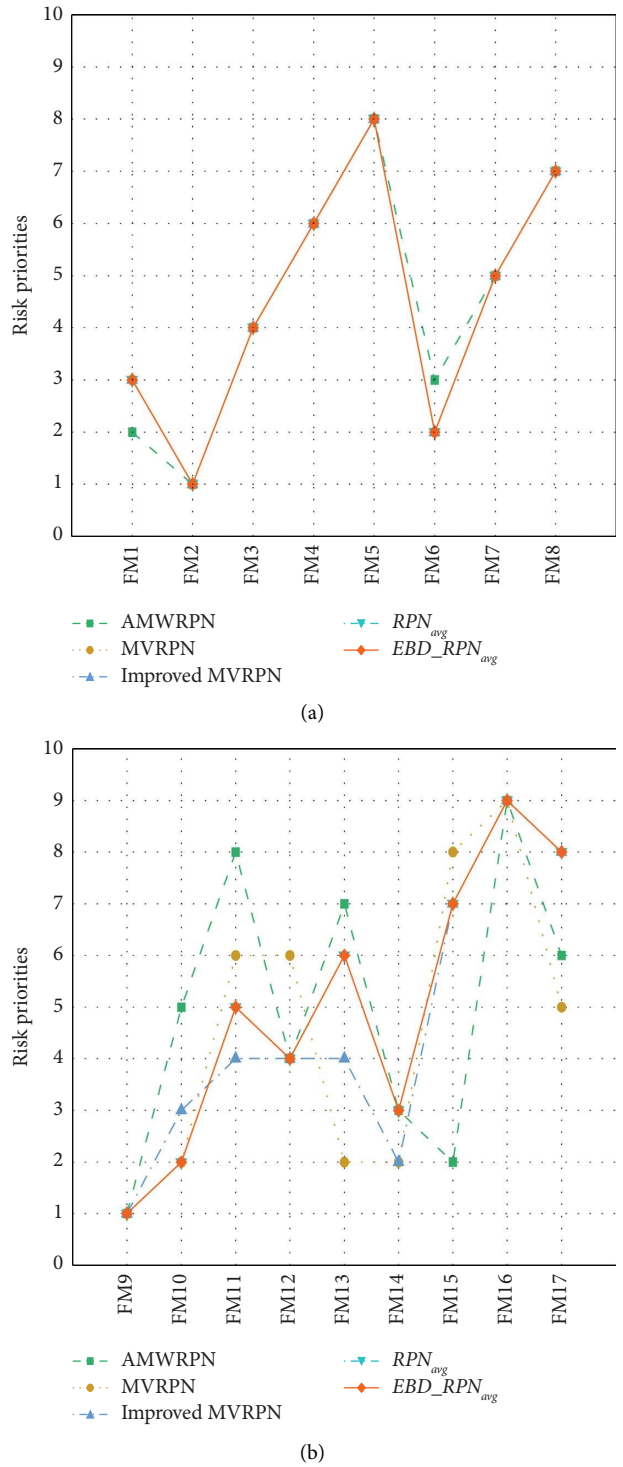

FIGURE 9: The risk ranking consequences of failure modes of rotor blades for an aircraft turbine. (a) Compressor rotor blades. (b) Turbo rotor blades.

The rank results of failure modes of rotor blades for an aircraft turbine are shown in Figure 9. In Figure 9(a), the risk priorities for compressor rotor blades by our method are nearly consistent with other methods. In Figure 9(b), the risk priorities for turbo rotor blades by our method completely coincide with the RPN_{avg}. Although the risk priorities by EBD_RPN_{avg} are slightly different with the three other methods, this is acceptable. It is the reason that the several identical RPN values, in the MVRPN method and the improved MVRPN method, lead to the sorting difference. Therefore, in the FMEA of the rotor blades of an aircraft turbine, the proposed method has effectiveness and practicality.

8. Conclusion

In this paper, an enhanced belief divergence, named as EBD, is proposed to measure the discrepancy between evidence. The proposed EBD can distinguish between singletons and multielement sets and express the intersection relationship among subsets. Some important properties of the EBD are inferred. In addition, the comparison interprets that the EBD has a preferable effect on conflict measurement. Next, an EBD-based multisource information fusion method is devised. In the applications of target recognition and iris classification, the proposed method can effectively handle uncertainty and conflict with higher accuracy values. Specially, the basic belief assignment of the true target in target recognition achieves 0.9904. Finally, in the risk priority evaluation of the failure modes of the rotor blades of an aircraft turbine, the risk ranking results by the proposed method are almost consistent with other methods, demonstrating the applicability of the proposed method.

In our future work, we intend to further study the performance of the proposed method to handle nonconflicting information. Also, we can broaden the proposed approach to solve other practical problems, such as image processing problems. Besides, we will deepen our research on fusion method when the BPA is an interval value.

Data Availability

The authors declare that all data supporting the findings of this study are included within the article.

Conflicts of Interest

The authors declare that there are no conflicts of interest.

Acknowledgments

This work is supported by the Fundamental Research Funds for the Central Universities (No. 2572023DJ04 and No. 2572018BC21).

Supplementary Materials

The three risk factors, occurrence (O), severity (S) and detection (D), use a numeric scale rating from 1 to 10, Tables S1–S3 in Supplementary Description offer the suggested criteria of rating for each risk factor of a failure in FMEA. (*Supplementary Materials*)

References

[1] J. W. Lai, J. Chang, L. Ang, and K. H. Cheong, "Multi-level information fusion to alleviate network congestion," *Information Fusion*, vol. 63, pp. 248–255, 2020.

[2] Z. Wu and H. Liao, "A consensus reaching process for large-scale group decision making with heterogeneous preference information," *International Journal of Intelligent Systems*, vol. 36, no. 9, pp. 4560–4591, 2021.

[3] E. Lefevre, O. Colot, and P. Vannoorenberghe, "Belief function combination and conflict management," *Information Fusion*, vol. 3, no. 2, pp. 149–162, 2002.

[4] X. Wang and Y. Song, "Uncertainty measure in evidence theory with its applications," *Applied Intelligence*, vol. 48, no. 7, pp. 1672–1688, 2018.

[5] A. P. Dempster, "Upper and lower probabilities induced by a multi-valued mapping," *The Annals of Mathematical Statistics*, vol. 38, no. 2, pp. 325–339, 1967.

[6] G. Shafer, "A mathematical theory of evidence," *Technometrics*, vol. 20, no. 1, p. 106, 1978.

[7] X. Chen and Y. Deng, "A new belief entropy and its application in software risk analysis," *International Journal of Computers, Communications and Control*, vol. 18, no. 2, 2023.

[8] Y. Pan, L. Zhang, Z. Li, and L. Ding, "Improved fuzzy Bayesian network-based risk analysis with interval-valued fuzzy sets and D-S evidence theory," *IEEE Transactions on Fuzzy Systems*, vol. 28, no. 9, pp. 2063–2077, 2020.

[9] D. Wu and Y. Tang, "An improved failure mode and effects analysis method based on uncertainty measure in the evidence theory," *Quality and Reliability Engineering International*, vol. 36, no. 5, pp. 1786–1807, 2020.

[10] L. Chang, L. Zhang, C. Fu, and Y.-W. Chen, "Transparent digital twin for output control using belief rule base," *IEEE Transactions on Cybernetics*, vol. 52, no. 10, pp. 10364–10378, 2022.

[11] X. J. Ma, M. N. Li, and J. F. Wang, "High-density impulse noise recognition algorithm based on D-S credibility weighted model," *Chinese Journal of Sensors and Actuators*, vol. 35, no. 6, pp. 769–777, 2022.

[12] J. X. Zhang, X. J. Ma, T. T. Song, A. Wang, and Y. H. Lin, "An enhanced pignistic transformation-based fusion scheme with applications in image segmentation," *IEEE Access*, vol. 11, pp. 19892–19913, 2023.

[13] C. Fu, W. Chang, and S. Yang, "Multiple criteria group decision making based on group satisfaction," *Information Sciences*, vol. 518, pp. 309–329, 2020.

[14] P. Liu, X. Zhang, and W. Pedrycz, "A consensus model for hesitant fuzzy linguistic group decision-making in the framework of Dempster–Shafer evidence theory," *Knowledge-Based Systems*, vol. 212, Article ID 106559, 2021.

[15] L. Xiong, X. Su, and H. Qian, "Conflicting evidence combination from the perspective of networks," *Information Sciences*, vol. 580, pp. 408–418, 2021.

[16] R. R. Yager, "On the Dempster-Shafer framework and new combination rules," *Information Sciences*, vol. 41, no. 2, pp. 93–137, 1987.

[17] D. Dubois and H. Prade, "Representation and combination of uncertainty with belief functions and possibility measures," *Computational Intelligence*, vol. 4, no. 3, pp. 244–264, 1988.

[18] X. Chen and Y. Deng, "A novel combination rule for conflict management in data fusion," *Soft Computing*, vol. 27, no. 22, pp. 16483–16492, 2023.

[19] W. Zhang and Y. Deng, "Combining conflicting evidence using the DEMATEL method," *Soft Computing*, vol. 23, no. 17, pp. 8207–8216, 2019.

[20] C. K. Murphy, "Combining belief functions when evidence conflicts," *Decision Support Systems*, vol. 29, no. 1, pp. 1–9, 2000.

[21] X. Gao and F. Xiao, "A generalized x^2 divergence for multisource information fusion and its application in fault diagnosis," *International Journal of Intelligent Systems*, vol. 37, no. 1, pp. 5–29, 2022.

[22] C. Zhu, F. Xiao, and Z. Cao, "A generalized Rényi divergence for multi-source information fusion with its application in EEG data analysis," *Information Sciences*, vol. 605, pp. 225–243, 2022.

[23] D. Han, J. Dezert, and Y. Yang, "Belief interval-based distance measures in the theory of belief functions," *IEEE Transactions on Systems, Man, and Cybernetics: Systems*, vol. 48, no. 6, pp. 833–850, 2018.

[24] C. Cheng and F. Xiao, "A distance for belief functions of orderable set," *Pattern Recognition Letters*, vol. 145, pp. 165–170, 2021.

[25] J. Deng, Y. Deng, and K. H. Cheong, "Combining conflicting evidence based on Pearson correlation coefficient and weighted graph," *International Journal of Intelligent Systems*, vol. 36, no. 12, pp. 7443–7460, 2021.

[26] H. Wang, X. Deng, W. Jiang, and J. Geng, "A new belief divergence measure for Dempster-Shafer theory based on belief and plausibility function and its application in multi-source data fusion," *Engineering Applications of Artificial Intelligence*, vol. 97, Article ID 104030, 2021.

[27] Z. Deng and J. Wang, "Measuring total uncertainty in evidence theory," *International Journal of Intelligent Systems*, vol. 36, no. 4, pp. 1721–1745, 2021.

[28] A.-L. Jousselme, D. Grenier, and E. Bossé, "A new distance between two bodies of evidence," *Information Fusion*, vol. 2, no. 2, pp. 91–101, 2001.

[29] R. Li, Z. Chen, H. Li, and Y. Tang, "A new distance-based total uncertainty measure in Dempster-Shafer evidence theory," *Applied Intelligence*, vol. 52, no. 2, pp. 1209–1237, 2022.

[30] Y. Cui and X. Deng, "Plausibility entropy: a new total uncertainty measure in evidence theory based on plausibility function," *IEEE Transactions on Systems, Man, and Cybernetics: Systems*, vol. 53, no. 6, pp. 3833–3844, 2023.

[31] F. Xiao, Z. Cao, and A. Jolfaei, "A novel conflict measurement in decision-making and its application in fault diagnosis," *IEEE Transactions on Fuzzy Systems*, vol. 29, no. 1, pp. 186–197, 2021.

[32] Z. Deng and J. Wang, "A new evidential similarity measurement based on Tanimoto measure and its application in multi-sensor data fusion," *Engineering Applications of Artificial Intelligence*, vol. 104, Article ID 104380, 2021.

[33] Y. Deng, W. K. Shi, Z. F. Zhu, and Q. Liu, "Combining belief functions based on distance of evidence," *Decision Support Systems*, vol. 38, no. 3, pp. 489–493, 2004.

[34] F. Xiao, "Multi-sensor data fusion based on the belief divergence measure of evidences and the belief entropy," *Information Fusion*, vol. 46, pp. 23–32, 2019.

[35] C. Zhu and F. Xiao, "A belief Hellinger distance for D–S evidence theory and its application in pattern recognition," *Engineering Applications of Artificial Intelligence*, vol. 106, Article ID 104452, 2021.

[36] M. C. Florea and E. Bossé, "Crisis management using Dempster Shafer theory: using dissimilarity measures to characterize sources's reliability," in *Proceedings of the Symposium on C3l for Crisis, Emergency and Consequence Management*, France, April, 2009.

[37] Y. Wang, K. Zhang, and Y. Deng, "Base belief function: an efficient method of conflict management," *Journal of Ambient Intelligence and Humanized Computing*, vol. 10, no. 9, pp. 3427–3437, 2019.

[38] D. Dubois and H. Prade, "A note on measures of specificity for fuzzy sets," *International Journal of General Systems*, vol. 10, no. 4, pp. 279–283, 1985.

[39] R. R. Yager, "Entropy and specificity in a mathematical theory of evidence," *International Journal of General Systems*, vol. 9, no. 4, pp. 249–260, 1983.

[40] Y. Deng, "Information volume of mass function," *International Journal of Computers, Communications and Control*, vol. 15, no. 6, 2020.

[41] F. Xiao, "A new divergence measure for belief functions in D–S evidence theory for multisensor data fusion," *Information Sciences*, vol. 514, pp. 462–483, 2020.

[42] Nancy and H. Garg, "A novel divergence measure and its based TOPSIS method for multi criteria decision-making under single-valued neutrosophic environment," *Journal of Intelligent and Fuzzy Systems*, vol. 36, no. 1, pp. 101–115, 2019.

[43] A. Bhattacharyya, "On a measure of divergence between two statistical populations defined by their probability distribution," *The bulletin of CMS*, vol. 35, pp. 99–110, 1943.

[44] B. Ristic and P. Smets, "The TBM global distance measure for the association of uncertain combat ID declarations," *Information Fusion*, vol. 7, no. 3, pp. 276–284, 2006.

[45] Q. Zhou and Y. Deng, "Handling uncertainty in view of inner product," in *Proceedings of the 2021 IEEE International Conference on Unmanned Systems (ICUS)*, pp. 305–308, IEEE, Beijing, China, October, 2021.

[46] B. Liu, Y. Deng, and K. H. Cheong, "An improved multisource data fusion method based on a novel divergence measure of belief function," *Engineering Applications of Artificial Intelligence*, vol. 111, Article ID 104834, 2022.

[47] R. R. Yager and F. Petry, "An intelligent quality-based approach to fusing multi-source probabilistic information," *Information Fusion*, vol. 31, pp. 127–136, 2016.

[48] C. Gini, "Variabilitae mutabilita," in *Reprinted in Memorie di Metodologica Statistica*, E. Pizetti and T. Salvemini, Eds., Libreria Eredi Virgilio Veschi, Rome, Italy, 1955.

[49] D. Li, Y. Deng, and K. H. Cheong, "Multisource basic probability assignment fusion based on information quality," *International Journal of Intelligent Systems*, vol. 36, no. 4, pp. 1851–1875, 2021.

[50] J. Qian, X. Guo, and Y. Deng, "A novel method for combining conflicting evidences based on information entropy," *Applied Intelligence*, vol. 46, no. 4, pp. 876–888, 2017.

[51] H. Wang, Y.-P. Fang, and E. Zio, "Risk assessment of an electrical power system considering the influence of traffic congestion on a hypothetical scenario of electrified transportation system in New York State," *IEEE Transactions on Intelligent Transportation Systems*, vol. 22, no. 1, pp. 142–155, 2021.

[52] J. Yuan, F. L. Wang, S. Wang, and L. P. Zhao, "A fault diagnosis approach by D-S fusion theory and hybrid expert knowledge system," *Acta Automatica Sinica*, vol. 43, no. 9, pp. 1580–1587, 2017.

[53] J. Yang, H.-Z. Huang, L.-P. He, S.-P. Zhu, and D. Wen, "Risk evaluation in failure mode and effects analysis of aircraft turbine rotor blades using Dempster–Shafer evidence theory

under uncertainty," *Engineering Failure Analysis*, vol. 18, no. 8, pp. 2084–2092, 2011.

[54] Y. Yuan and Y. Tang, "Fusion of expert uncertain assessment in FMEA based on the negation of basic probability assignment and evidence distance," *Scientific Reports*, vol. 12, no. 1, Article ID 8424, 2022.

[55] Y. Tang, D. Zhou, and F. T. S. Chan, "AMWRPN: ambiguity measure weighted risk priority number model for failure mode and effects analysis," *IEEE Access*, vol. 6, pp. 27103–27110, 2018.

[56] X. Su, Y. Deng, S. Mahadevan, and Q. Bao, "An improved method for risk evaluation in failure modes and effects analysis of aircraft engine rotor blades," *Engineering Failure Analysis*, vol. 26, pp. 164–174, 2012.